B038347

DETERMINATION OF THE MECHANICAL PROPERTIES OF AIRCRAFT-STRUCTURAL MATERIALS AT VERY HIGH TEMPERATURES AFTER RAPID HEATING

James B. Preston

J. Robert Kattus

Southern Research Institute

AD ⊃ 37 ⅔ ⅔

APRIL 1960

WRIGHT AIR DEVELOPMENT DIVISION

NOTICES

When Government drawings, specifications, or other data are used for any purpose other than in connection with a definitely related Government procurement operation, the United States Government thereby incurs no responsibility nor any obligation whatsoever; and the fact that the Government may have formulated, furnished, or in any way supplied the said drawings, specifications, or other data, is not to be regarded by implication or otherwise as in any manner licensing the holder or any other person or corporation, or conveying any rights or permission to manufacture, use, or sell any patented invention that may in any way be related thereto.

– – – – –

Qualified requesters may obtain copies of this report from the Armed Services Technical Information Agency, (ASTIA), Arlington Hall Station, Arlington 12, Virginia.

– – – – –

This report has been released to the Office of Technical Services, U. S. Department of Commerce, Washington 25, D. C., for sale to the general public.

– – – – –

Copies of WADC Technical Reports and Technical Notes should not be returned to the Wright Air Development Center unless return is required by security considerations, contractual obligations, or notice on a specific document.

A D   2 ?   7 ? 7

DETERMINATION OF THE MECHANICAL PROPERTIES OF AIRCRAFT-STRUCTURAL MATERIALS AT VERY HIGH TEMPERATURES AFTER RAPID HEATING

James B. Preston
J. Robert Kattus

Southern Research Institute

APRIL 1960

FOREWORD

This report was prepared by Southern Research Institute under USAF Contract No. AF 33(616)-3494. The contract was initiated under Project No. 2998, Task No. 73320, "Development and Evaluation of Materials for ICBM and IRBM Applications." The work was administered under the direction of the Materials Laboratory, Directorate of Laboratories, Wright Air Development Center, with Mr. R. F. Klinger acting as project engineer.

This report covers work conducted from May 1957 through June 1959.

In addition to the authors, the following personnel at Southern Research Institute contributed significantly to the project:

1. F. R. O'Brien, Assistant Director
2. Willis Burks and Edward Rohrbach, who assisted in the development and maintenance of the equipment and carried out some of the testing.
3. Jack S. Barr, who carried out most of the work involving thermal gradients.
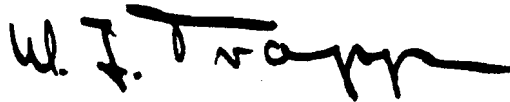4. Walter Rogers, who assisted in the testing.

ABSTRACT

Structural components in high-speed aircraft and in missiles must function for short periods of time at high temperatures and at high stresses, and frequently the heating and loading occur simultaneously. The requirement for reliability without overdesign demands accurate test data obtained under conditions approximating the expected operating conditions. In an effort to fulfill a portion of this need, this program was divided into four independent areas of work as follows: (1) The tensile properties of unalloyed beryllium were determined at test temperatures from ambient through 1500° F. (2) The short-time, elevated-temperature tensile properties were determined for ten combinations of base materials and coating materials (Cr-Ni electroplate on copper sheet, Rokide A on copper sheet, Rokide Z on copper sheet, Rokide ZS on copper sheet, Cr electroplate on A-nickel sheet, Ni-Cr electroplate on molybdenum sheet, Rokide Z on molded graphite, Rokide ZS on molded graphite, Crystalon C on molded graphite and SiC-SiN on molded graphite). (3) The effects of linear thermal gradients up to 1500° F/in. on the tensile properties of a typical refractory alloy were investigated. (4) The effects of simultaneous heating and loading on the tensile properties of a typical structural alloy were investigated. This report covers the first three of these four areas of work; a supplementary report will be issued shortly containing all of the results of the investigations involving simultaneously transient temperature and load.

PUBLICATION REVIEW

This report has been reviewed and is approved.

FOR THE COMMANDER:

W. J. Trapp
Chief, Strength and Dynamics Branch
Metals and Ceramics Division
Materials Laboratory

TABLE OF CONTENTS

LIST OF ILLUSTRATIONS

LIST OF TABLES

LIST OF TABLES (Cont'd)

DETERMINATION OF THE MECHANICAL PROPERTIES OF AIRCRAFT-STRUCTURAL MATERIALS AT VERY HIGH TEMPERATURES AFTER RAPID HEATING

SECTION I. INTRODUCTION

1.1 Purpose of the Program

Modern high-speed aircraft and missiles often operate under conditions that subject parts of the structure and of the power plant to rapid loading and to rapid heating to temperatures approaching the melting points of the materials involved. Frequently heating and loading occur simultaneously. Because of the higher operating speeds and severe operating conditions, new design criteria have been applied to certain components of high-speed aircraft and missiles in order to utilize the marginal strength of the materials. But the requirement for reliability without overdesign demands accurate test data obtained under conditions approximating the expected operating conditions of the component. Until recently almost all of the available test data on mechanical properties were applicable to the more conservatively designed structures.

The purpose of the overall program, which has spanned two research contracts and 3 1/2 years, was to determine the mechanical properties of several promising materials under conditions intended to simulate roughly some of the operating conditions of high-speed aircraft and missiles. This report covers the work that was conducted during the period from May 1957 through June 1959. This work was divided into four unrelated areas of evaluation—(1) the determination of the tensile properties of unalloyed beryllium at test temperatures from ambient to 1500° F, (2), the evaluation of the effects of ten different protective coatings on the short-time, elevated-temperature tensile properties of four different base materials, (3) the determination of the effects of linear thermal gradients on the tensile properties of a high-temperature alloy, and (4) the determination of the effects of simultaneous heating and loading on the tensile properties of a high-temperature alloy. The technical portion of this report will be divided into three major sections corresponding to the first three of the four areas of work. Because the work on simultaneous heating and loading was extended beyond the termination of the other three areas of work, a separate supplementary report will be issued shortly containing all of the results of the investigation of the effects that simultaneously transient temperature and load produce on

tensile properties. Each section will contain the complete discussions of the scope, the test equipment peculiar to that area of work, the test results, and the conclusions pertaining to that one area of work.

1.2 History of the Program

Under the sponsorship of the Air Force, Southern Research Institute has carried out several programs of high-speed, high-temperature determinations of mechanical properties on aircraft-structural materials. During the first of such programs, which was begun in 1953 under Contract No. AF 33(616)-424, most of the basic test equipment and test methods were developed. An account of the development program and a description of the basic test equipment are contained in WADC Technical Report 55-199 Parts 1, 2, and 3. During the period of March 1955 through October 1955, several new materials and higher test temperatures were introduced in a brief program conducted under Contract No. AF 33(616)-2837. A second high-speed tensile machine and a short-time creep machine were constructed. This work was reported in WADC Technical Report 55-391. In March 1956 the first phase of the work was begun under Contract No. AF 33(616)-3494, extending the test conditions for most of the same materials that were tested under AF 33(616)-2837. This initial phase lasted eighteen months and was reported in WADC Technical Report 57-649 Part I. The second phase of the work under AF 33(616)-3494, which began in May 1957, is the subject of this report.

SECTION II. THE BASIC TEST EQUIPMENT

2.1 Background

This evaluation program began with a complete tensile testing equipment that had been developed during previous work sponsored by the Air Force. This test equipment was capable of recording stress-strain curves from tensile tests conducted at strain rates ranging from 0.00005 to 1.0 in./in./sec and at specimen temperatures ranging from ambient to the melting point of any metal or alloy. Strain was measured at the 2-in. gage points in all tests up to 3200° F and was measured at the crosshead in tests above 3200° F. A controlled source of electric power was used to heat the test specimens resistively from room temperature to any predetermined test temperature within 10 sec and, thereafter, to hold the test temperature constant within ±10° F for the duration of the test.

A brief description of each section of the test equipment follows; a complete discussion can be found in WADC Technical Report 57-649 Part I. Wherever modifications were made to the test equipment in order to perform some phase of the work being reported, those modifications are described in the section pertaining to that phase.

2.2 Loading the Specimen

The test specimens were loaded in tension by a screw-driven high-speed tensile machine with a load capacity of 5000 lb. The loading screw was coupled to the drive through an electromagnetic clutch. The drive consisted of (1) an adjustable-speed dc motor with a speed range of 20 to 1, (2) one of four interchangeable speed-reducers providing a selection of gear ratios between the motor and the screw from 1:1 to 2880:1, and (3) a large flywheel to absorb the shock of loading at very high speeds. Loading was initiated by electrically engaging the clutch to almost instantaneously start the cross-head moving at constant speed. By selecting the proper motor speed and gear ratio, the specimens could be loaded at strain rates from 0.00005 to 1.0 in./in./sec. Figure 1 is an assembly drawing showing the general arrangement of the components in the high-speed tensile machine.

2.3 Measuring and Recording Stress and Strain

Both the load cell and the extensometer used resistance strain gages as the basic sensing elements. In each transducer, two type SR-4 strain gages were mounted so that they were strained in tension, and two were mounted so that they were strained in compression. The four strain gages were connected in a bridge circuit, which was excited with 1 volt at 5000 cps. The resulting signals, proportional to stress and to strain in the gage section of the specimen, were amplified, demodulated, and applied to the X- and the Y-axes of a cathode-ray oscilloscope. A Polaroid-Land camera photographed the stress-strain curves traced out on the face of the cathode-ray tube. Figure 2 shows a functional block diagram of the recording and control equipment associated with the high-speed tensile machine.

One of the modifications to the original test equipment was the addition of a second extensometer and a second strain channel in the amplifier so that during each tensile test two stress-strain curves could be simultaneously recorded—one with high strain-magnification to show only to the yield point and one with low strain magnification to show the complete stress-strain relationship to fracture. In addition to the high-magnification clip-on extensometer at the gage points of the specimen, a low-magnification extensometer
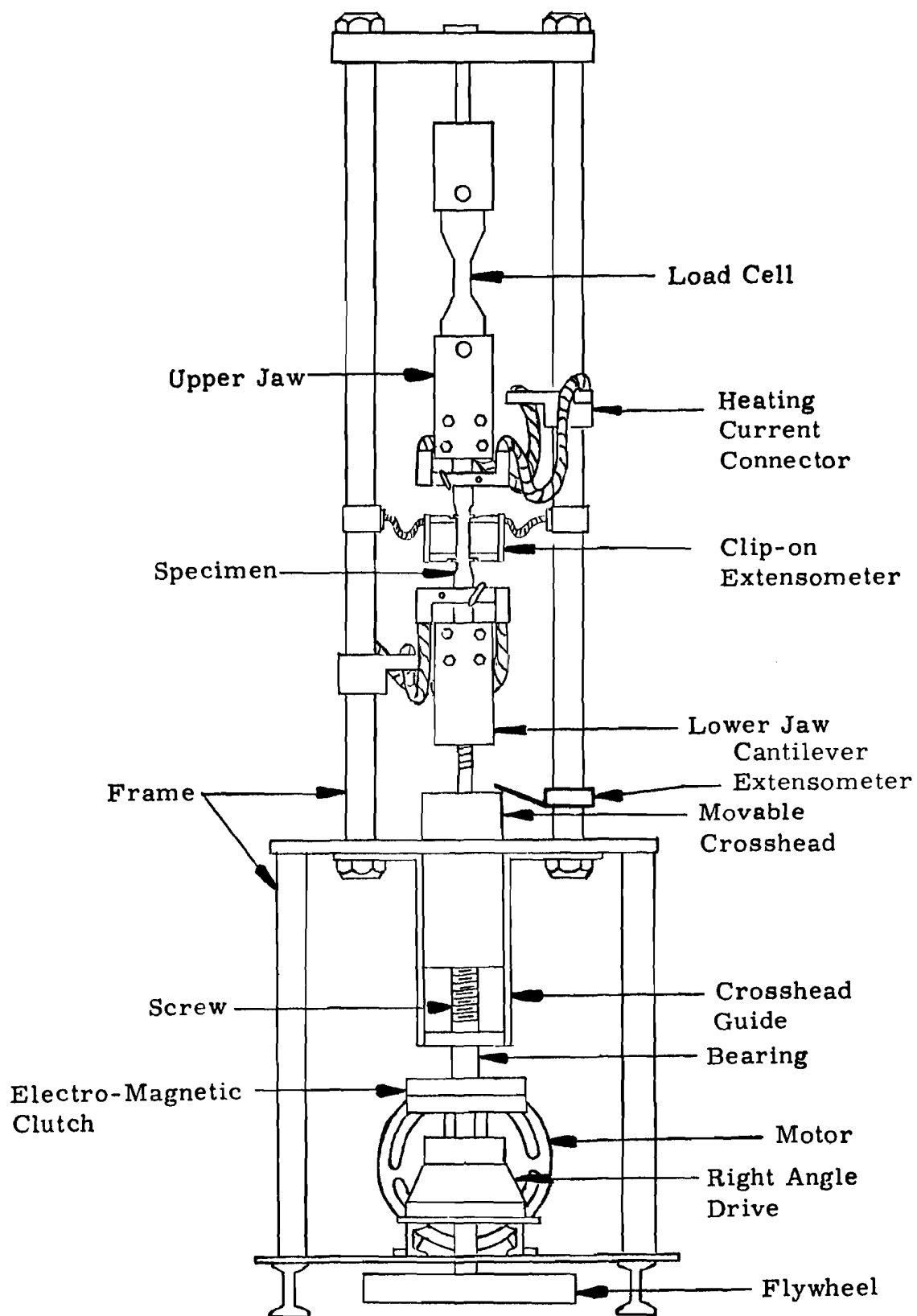
Figure 1. Arrangement of tensile loading machine.
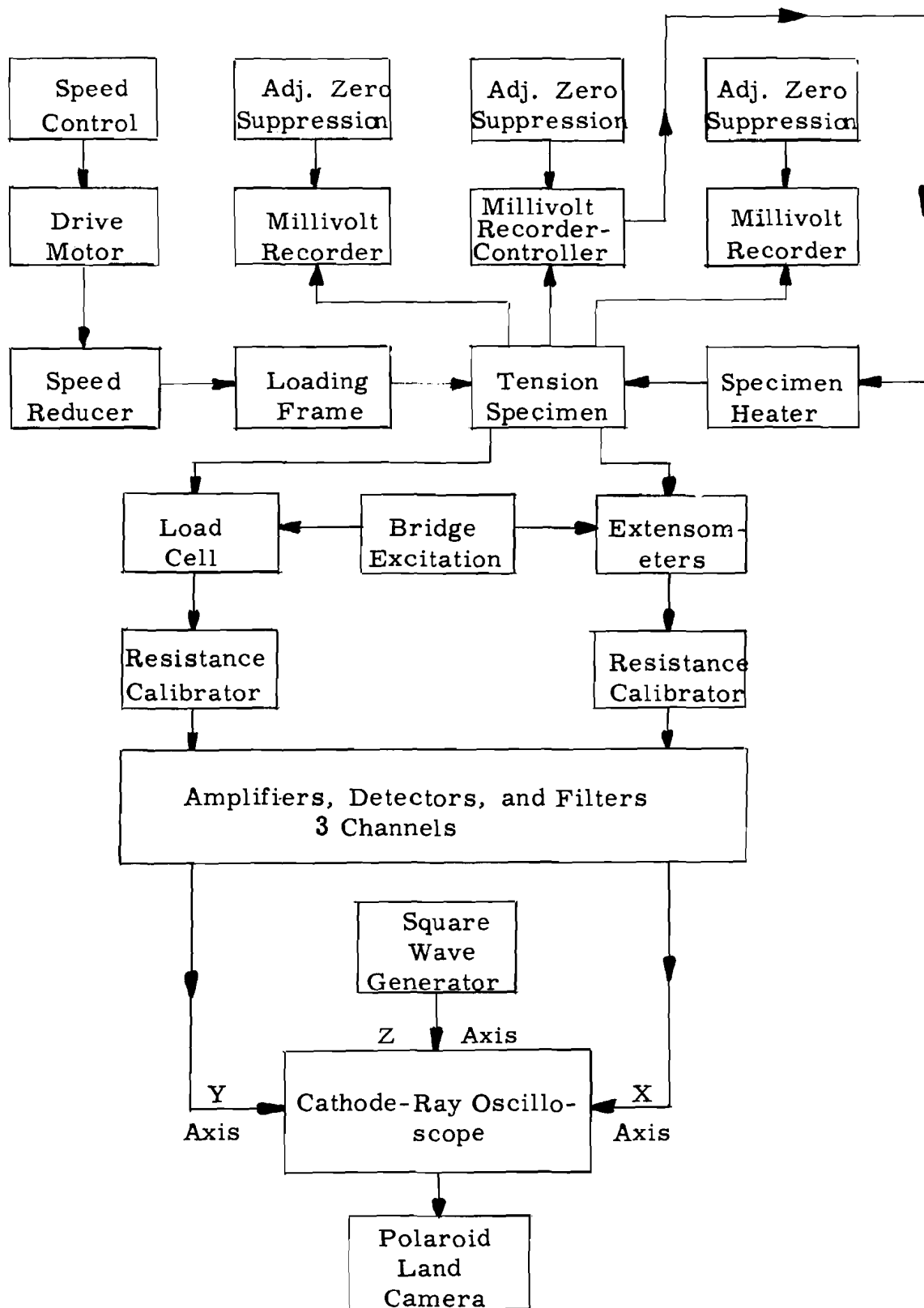
Figure 2. Functional block diagram of the recording and control equipment in the high-speed tensile machine.

was arranged to be actuated by the moving crosshead of the tensile machine. An additional channel was provided in the amplifier, and the two strain signals were combined in an electronic switch on a 50:50 time-shared basis. The composite strain signal of the electronic switch was fed to the X-axis input of the cathode-ray oscilloscope. The load signal was applied to the Y-axis as usual. The spot on the face of the cathode-ray oscilloscope would trace alternately a small segment of the elastic stress-strain curve and a small segment of the complete stress-strain curve. The switching rate of the electronic switch was synchronized by the square wave generator that formerly modulated the intensity of the cathode-ray beam to indicate time.

2.4 Measuring and Controlling the Test Temperature

The test specimens were heated by their own resistance to the passage of an electric current. A specially wound transformer was used to supply up to 1500 amperes of 60 cycle current to the specimens. Several taps on the primary of the transformer provided a coarse adjustment of the heating current. Accurate control of the temperature of the specimen was maintained through closer regulation of the heating current by a saturable reactor with its associated control circuit, which was described in WADC TR 57-649 Part I. During the course of the work covered in this report, the saturable reactor was replaced by a thyratron control to speed up the response of the control system so that it could produce rapid heating rates up to 2000 F/sec, and could produce other predetermined cycles of temperature vs. time.

The revised heating unit, which can be seen on the right side of the photograph in Figure 3, contains the complete servo temperature control and power supply within one cabinet. A millivolt input signal from the thermocouple commands the power supply to continuously regulate the current in the resistively heated specimen and to hold the temperature within $\pm$ 1/2% at any preset value within the practical range of thermocouples. At higher temperatures, a radiation pyrometer can be substituted for the thermocouple with just as good reproducibility but with an accuracy dependent upon the calibration of the pyrometer.

A schematic wiring diagram of the new specimen heating unit is shown in Figure 4. The method of measuring and indicating the test temperature was the same as that of the old heating unit—a No. 36 chromel-alumel (or platinum-platinum 10% rhodium) thermocouple welded to the center of the specimen and a Speedomax potentiometer with adjustable range and adjustable zero suppression. The range was usually set for 0-10 mv full scale and the zero suppression was set for each test temperature so that the control
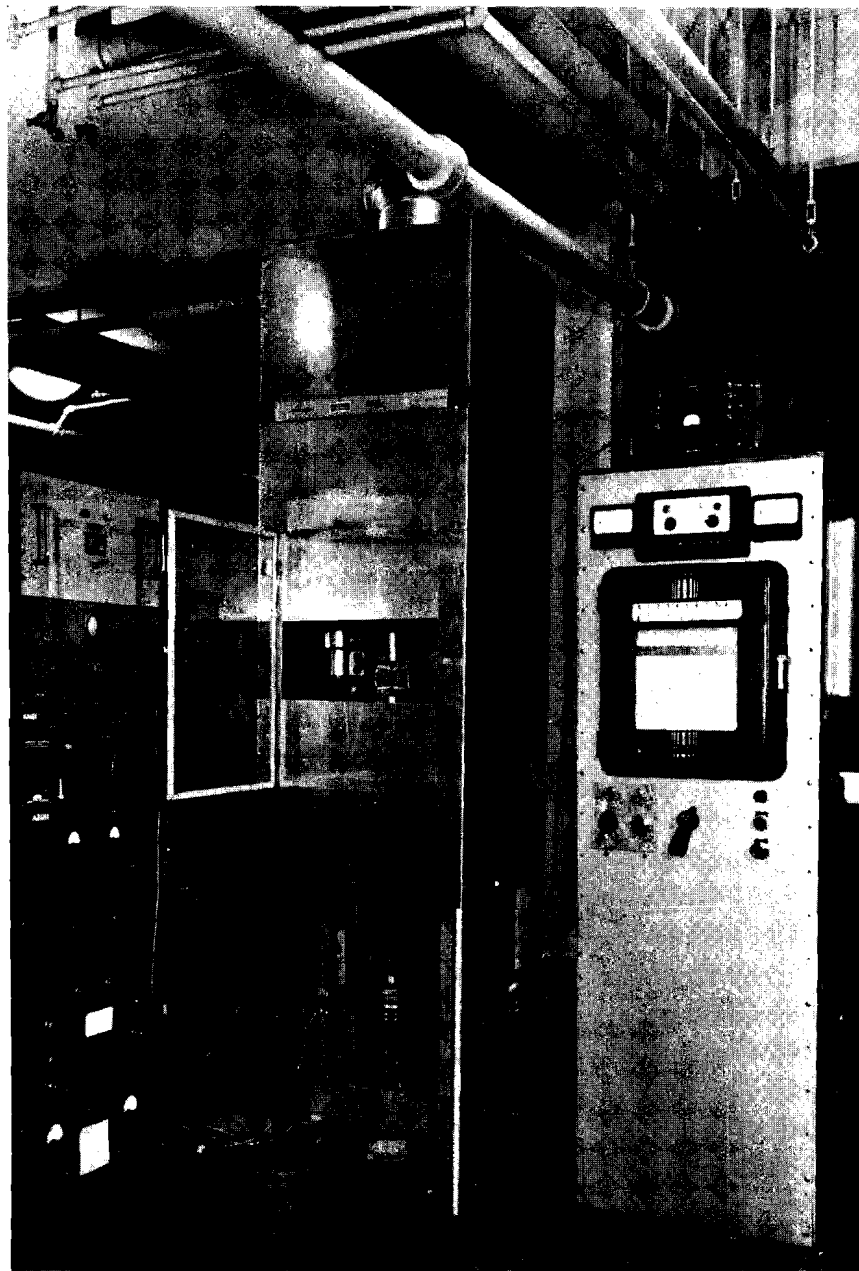
Figure 3. High-speed tensile testing equipment with the fume hood over the loading frame (center) for the evaluations of beryllium. The stress-strain recording equipment and the control panel is at the left; the controlled power-supply for resistance heating is at the right.

20 kva Transformer

Sec Amps

Test Specimen

CR

CR

Tap Switch

15V

230 V
60 Cycle
Line

Heat
Start

Heat
Stop

T. C.

230 V

CR

CR

230 V

Speedomax
Potentiometer

Control Slidewire

16-amp
Thyratrons

600 V

Pri
Amps

Thyrapulse
Firing Angle
Shifter

L & N Series 60
CAT.
Control Unit
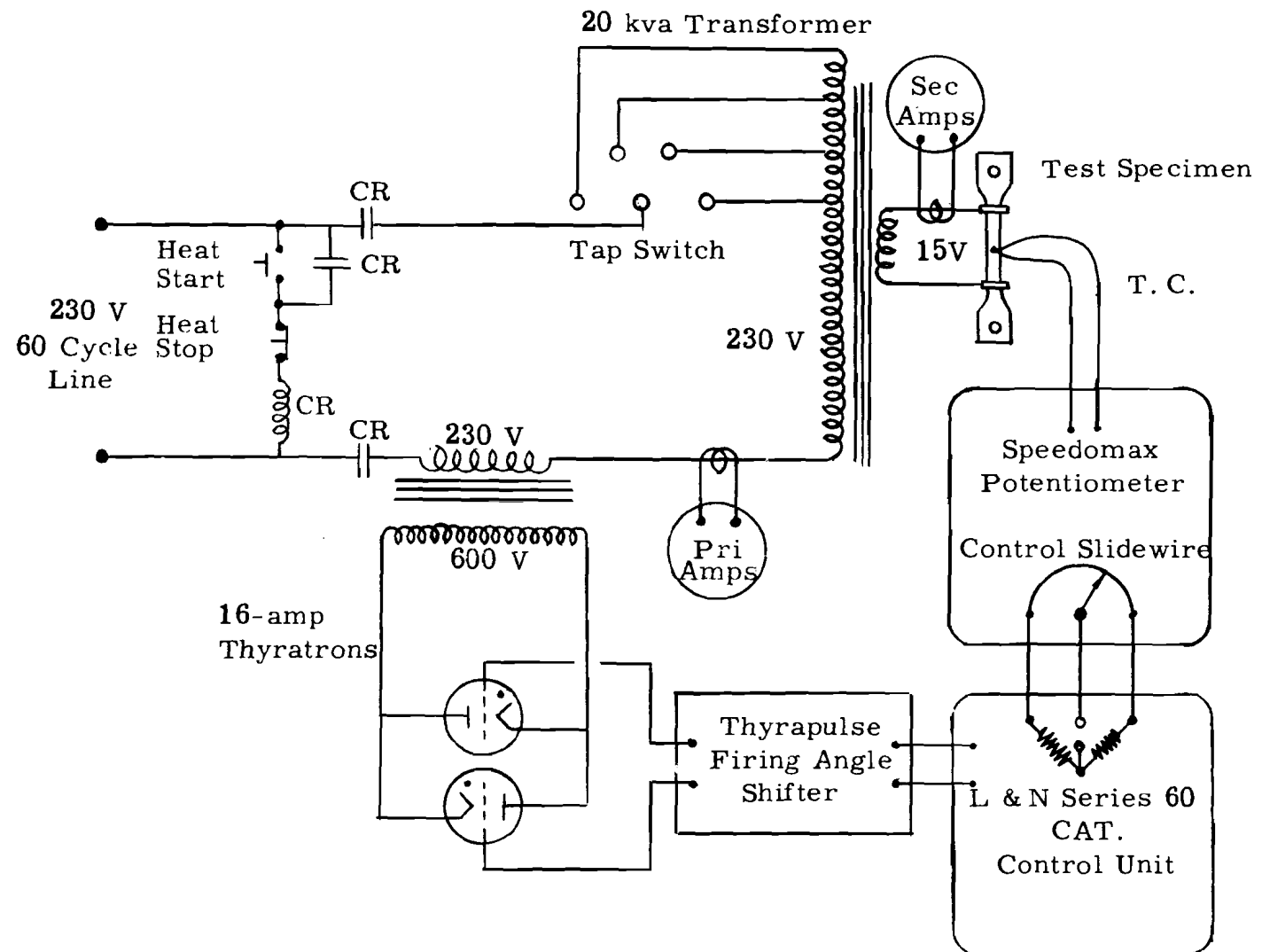
Figure 4. Schematic wiring diagram of temperature-control servo for
resistance-heated test specimens.

temperature would be indicated at the midpoint of the scale. A control slide-wire was added to the Speedomax potentiometer so that the position of the slider along the slidewire was directly proportional to the indicated tempera-ture on the scale of the instrument. In conjunction with two equal fixed resistors in the control unit, the control slidewire formed half of a bridge circuit, which was the temperature-error detector. When the potentiometer indicator was on the midscale control point, the bridge was balanced, and the error signal was zero. When the indicated temperature exceeded the control point, the bridge was unbalanced so that a positive error signal was produced, and, conversely, when the indicated temperature was below the control point, a negative error signal was produced. In the Leeds and Northrup Series 60 Control Unit, the error signal was processed through an amplifier and stabilizing networks, which generate adjustable amounts of rate and reset action to stabilize the system. The electrical output of the Control Unit increases whenever the error signal is negative, decreases whenever the error signal is positive, or maintains a constant value whenever the error signal is zero. The Thyrapulse is a packaged electromagnetic grid-circuit for thyratrons, which converts the dc output from the Control Unit into voltage pulses at 60 cps to fire the thyratrons. As the output from the Control Unit varies from 0 to 100%, the electrical angle of the pulses with respect to line voltage varies from 180° to 0° causing the conduction cycle of the thyratrons to vary from 0 to 100%. The 230/600 volt transformer is an impedance-matching device to enable the thyratrons to control over 2 1/2 times more power than would be possible with the same tubes directly in series with the line and the load. The heating current is supplied to the test specimen from a 230 volt, 60 cycle line through a 20 kva step-down transformer. The thyratrons in the primary regulate the heating current in the test specimen, and thereby, close the loop in the servo temperature control.

To summarize the operation: the thermocouple and the potentiometer continuously monitor the temperature and the temperature-error of the specimen. The Control Unit and the thyratron circuit are directed by the temperature-error signal to continuously and almost instantaneously adjust the heating current in the direction of reducing the temperature-error to zero.

SECTION III. THE TENSILE PROPERTIES OF BERYLLIUM

3.1 Scope

A limited investigation was conducted to determine the tensile properties of unalloyed beryllium. The beryllium bars, from which the test specimens were machined, contained a minimum of 98% beryllium, the major impurity being oxygen. A total of 25 test specimens were furnished by AVCO Manufacturing Corporation. These test specimens, pictured in Figure 5, had gage sections 2-in. long and 0.20-in. diameter with threaded shoulders 0.375-in. diameter.

Tensile tests were performed in atmospheres of air and argon at room temperature, 500° F, 1000° F, and 1500° F. The specimens were heated to test temperature within 20 sec, held at test temperature for 10 sec, and then loaded to failure at nominal strain rates of 1.0 and 0.001 in./in./sec, both of which are relatively fast rates in comparison to normal testing procedures. Because of the limited number of specimens available, only one test was conducted at most of the test conditions. Although it was originally intended to test beryllium at 2000° F, these tests could not be carried out because of the need to check some scattered results in the data obtained at lower temperatures and because of the scarcity of specimens.

3.2 Special Test Equipment

All of the basic test equipment that had been developed in the prior phases of the work was suitable for the determination of the tensile properties of beryllium. A fume hood with forced draft was constructed to fit closely over the upper half of the high-speed tensile machine to remove any toxic fumes that might be given off by the beryllium at eleved temperature. The hood, which was constructed of light-weight aluminum sheet, was fitted with a hinged glass window for visibility during the test and for access to change specimens. Disposable filters removed most of the airborne particles before the discharge from the hood was released out-of-doors. At the maximum test temperature up to 1500° F the oxidation of the beryllium was very slight, but, if a maximum temperature of 2000° F had been used as planned, the hazzard would have been much greater due to the rapid oxidation of the beryllium. The hood in place over the tensile machine can be seen at the center in the photograph of Figure 3.
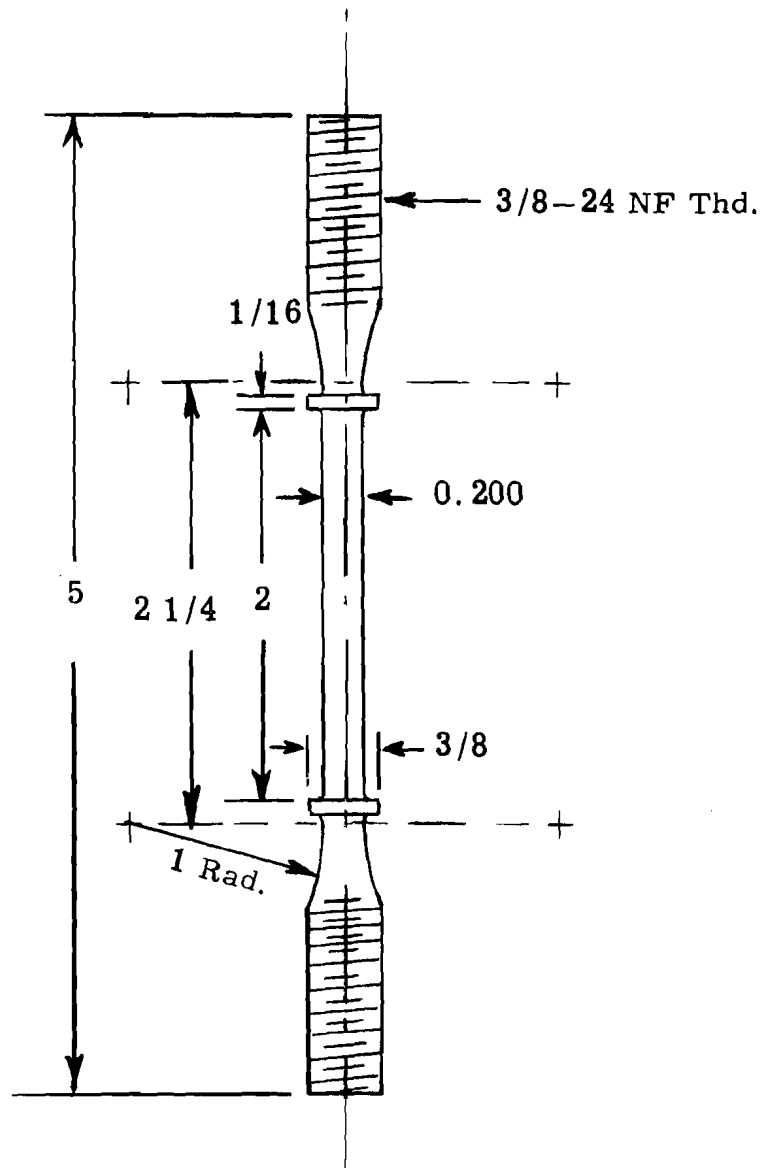
Figure 5. Beryllium tensile specimen

3.3 Results and Discussion

The results of the tensile tests on beryllium are tabulated in Table I for an atmosphere of air and in Table II for an atmosphere of argon. These tensile properties are plotted as functions of temperature in Figure 6 through 9. Each graph contains four curves to represent the four combinations of the two strain rates and two atmospheres. Figures 6 and 7 show, respectively, the effect of temperature upon the ultimate tensile strength and upon the 0.2%-offset yield strength of beryllium. Figure 8 shows the effect of temperature upon the modulus of elasticity, and Figure 9 shows the effect of temperature upon the percent elongation in the 2 in. gage length.

Before any conclusions are drawn from the data obtained in this work, several factors contributing to the scatter of the results should be mentioned. The data are statistically unrepresentative because of the limited number of specimens available for testing. The initial portion of the stress-strain curves for beryllium were rounded making it difficult to determine the initial slope, which represents the modulus of elasticity. A tangent line near the origin of the stress-strain curve was used to estimate the modulus values. Beryllium is extremely brittle in comparison to most metals. In almost any kind of mechanical test, a slight misalignment in loading or certain geometrical irregularities can cause a stress concentration at some point in the specimen. In most metals, a slight plastic flow in the affected area relieves such undesirable stress concentrations with very little damage to the rest of the section. But in such brittle metal as beryllium, the lack of ductility results in an early local fracture at any point of stress concentration, and this local fracture quickly propagates across the entire section at a nominal stress level below the ultimate stress. The tendency for materials to fail in this manner of brittle fracture increases with decreasing ductility and with increasing strain rate. The reason for the effect of strain rate is probably that plastic flow is time dependent—the slower the strain rate the greater the opportunity for plastic flow to relieve stress concentrations. Although it has been shown in earlier work on ductile materials that the lugs or rings, which are used to actuate an extensometer, at the gage points of tensile specimens have a negligible effect on the mechanical-property determinations, the use of rings on the beryllium specimen appears now to have been an inappropriate choice because of the slight stress-concentrating effect of these irregularities in the contour of the specimen. Most of the beryllium specimens broke in the vicinity of the rings rather than near the center of the gage section.

3.4 Conclusions

Figure 6 shows that, in general, the values of ultimate-tensile strength obtained at room temperature were lower than those obtained at some

Table I

Tensile Properties of Unalloyed Beryllium Bar at Different Temperatures
and Strain Rates in an Atmosphere of Air

All Specimens Heated to Test Temperature Within 20 Sec

Temp, °F	Time at Temp, Sec	Strain Rate, in. /in. /sec	0.2%-Offset Yld. Str.	Ultimate Str.	Mod. Elast., 10^6 psi	Elong., %
			1000 psi			
RT	–	0.00018	26.9	29.0	36.0	0.25
RT	–	–	28.8	30.4	43.9	0.25
RT	–	0.0056	23.0	26.5	31.5	0.25
RT	–	0.0013	–[1]	19.5	30.8	0.0
Avg.			26.2	28.6	35.6	0.0
500	10	0.0026	19.8	28.7	29.5	1.5
500	10	0.0026	22.3	30.1	28.6	2.5
Avg.			21.1	29.4	29.1	2.0
1000	10	0.0025	14.15	19.15	25.7	6.5
1000	10	0.0022	16.5	21.2	21.5	7.0
Avg.			15.3	20.2	23.6	6.75
1500	10	0.0013	8.5	8.84	19.8	2.0
RT	–	0.333	–[1]	10.95	34.7	0.0
RT	–	–	–[1]	7.48	25.1	0.0
RT	–	–	–[1]	16.5	38.7	0.0
RT	–	–	–[1]	15.9	48.6	0.0
Avg.				12.7	36.3	0.0
500	10	0.437	–[1]	11.55	26.7	0.0
1000	10	0.78	11.7	20.0	16.1	3.5
1500	10	1.126	8.83	11.3	7.0	3.0

1. Fractured before reaching 0.2% offset.

Table II

Tensile Properties of Unalloyed Beryllium Bar at Different Temperatures and Strain Rates in an Atmosphere of Argon

All Specimens Heated to Test Temperature Within 20 Sec

Temp, °F	Time at Temp, Sec	Strain Rate, in./in./sec	0.2%-Offset Yld. Str. (1000 psi)	Ultimate Str. (1000 psi)	Mod. Elast., 10^6 psi	Elong., %
500	10	0.00245	20.79	31.4	39.6	3.0
500	10	0.0027	25.2	32.8	20.0	1.5
Avg.			23.0	32.1	29.8	2.25
1000	10	0.0035	16.1	20.3	13.2	6.5
1500	10	0.00396	7.24	7.35	12.0	1.5
1500	10	0.003	6.94	7.85	12.0	1.5
Avg.			7.09	7.60	12.0	1.5
500	10	1.13	9.27	19.1	23.3	1.5
1000	10	0.59	15.1	20.2	21.2	4.5
1500	10	0.773	10.12	12.8	13.6	3.0
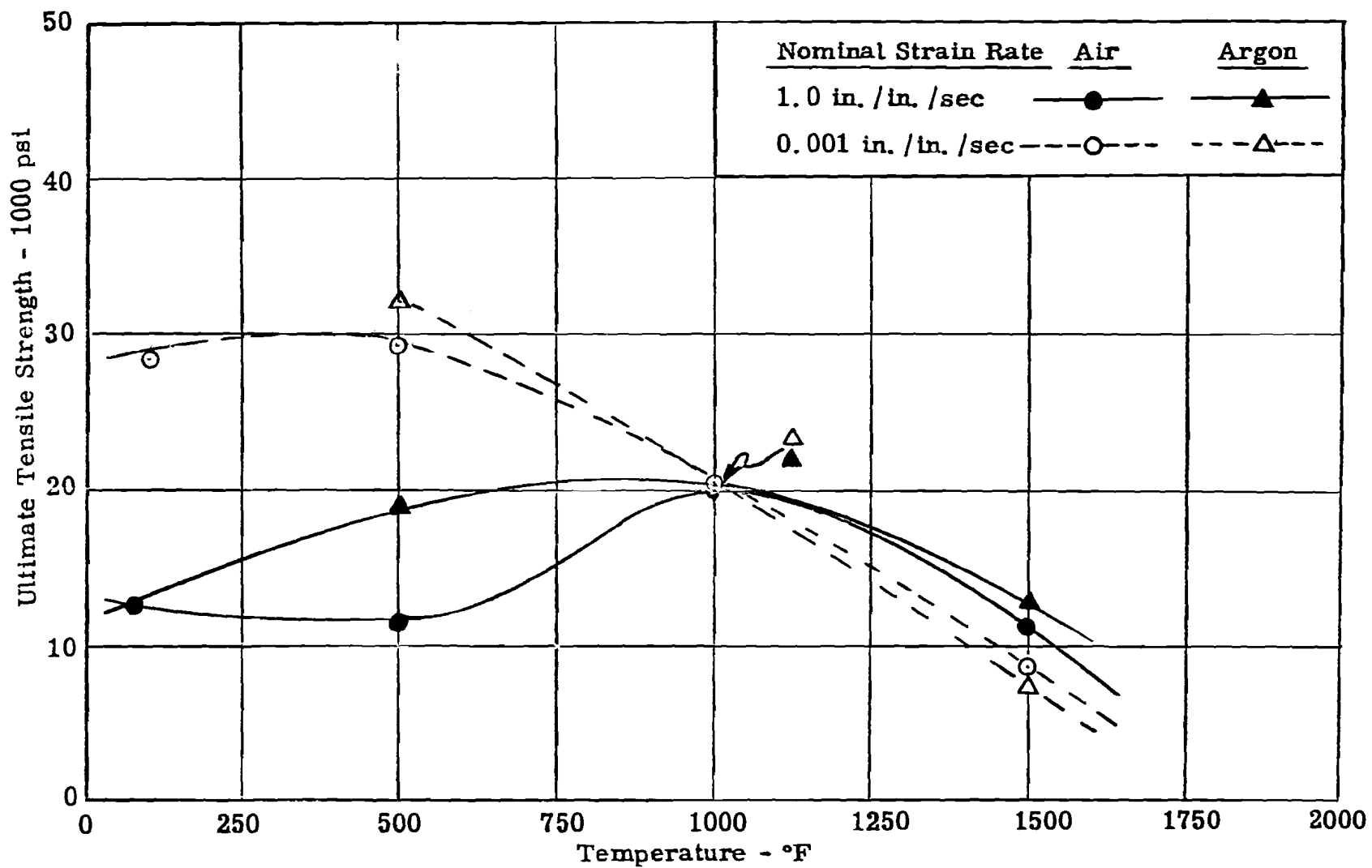
Figure 6.   Effect of temperature on the ultimate tensile strength of unalloyed beryllium
bar at two strain rates in atmospheres of air and of argon.
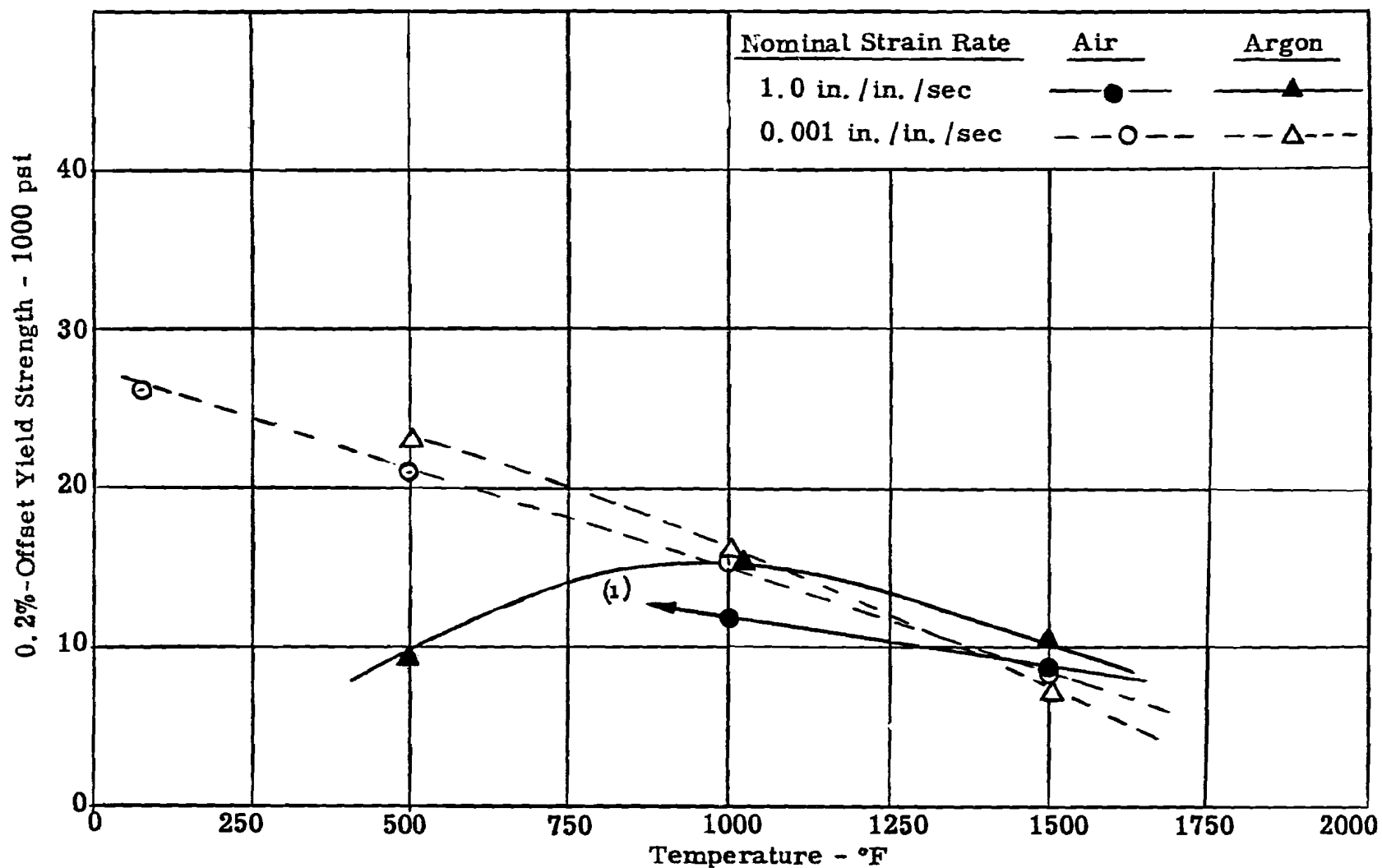
Figure 7. Effect of temperature on the 0. 2%-offset yield strength of unalloyed beryllium bar at two strain rates in atmospheres of air and of argon.

---

1 At strain rate of 1.0 in. /in. /sec and temperatures below 1000° F, most specimens broke before 0. 2% offset was reached.
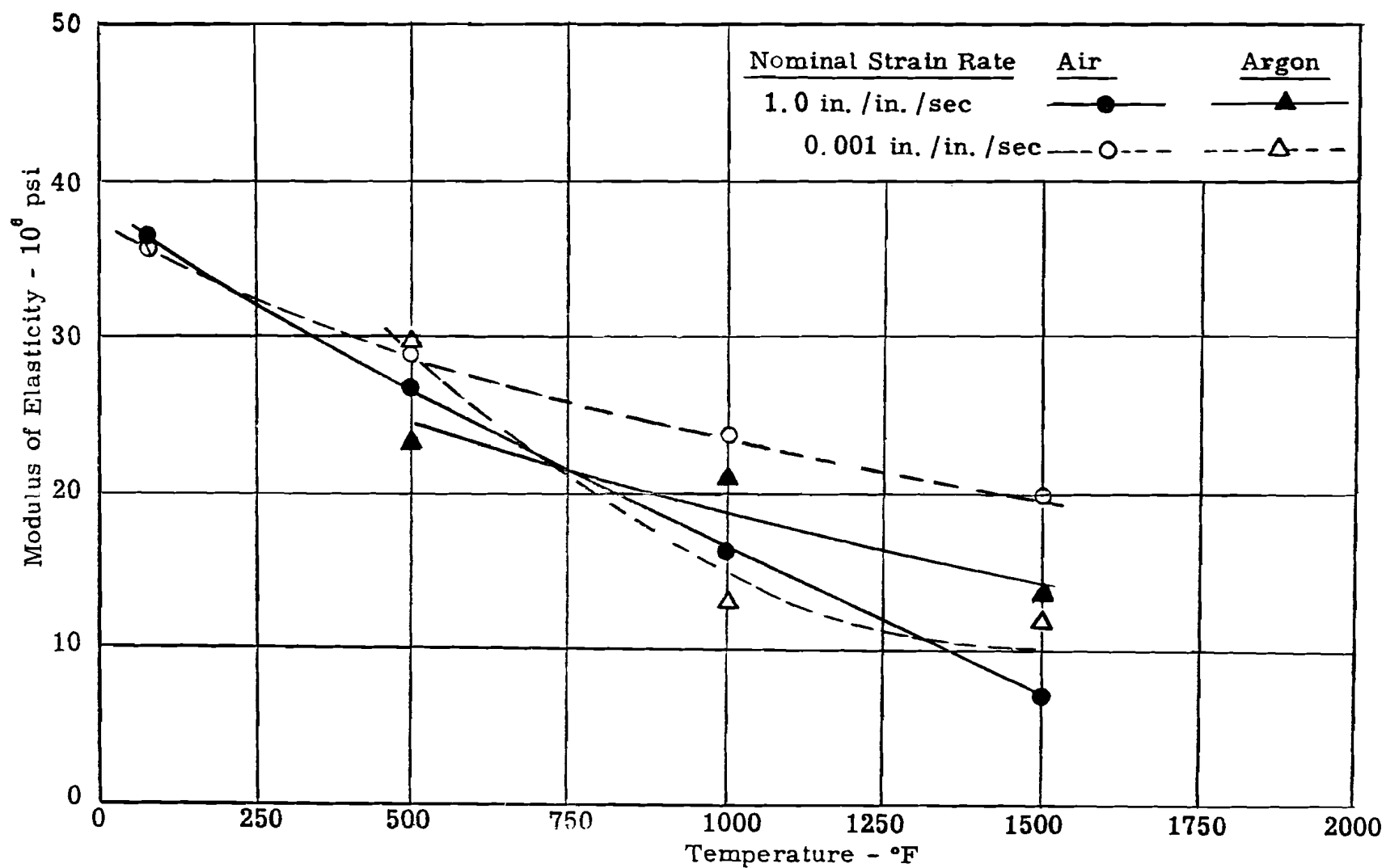
Figure 8.   Effect of temperature on the modulus of elasticity of unalloyed beryllium bar at two strain rates in atmospheres of air and of argon.
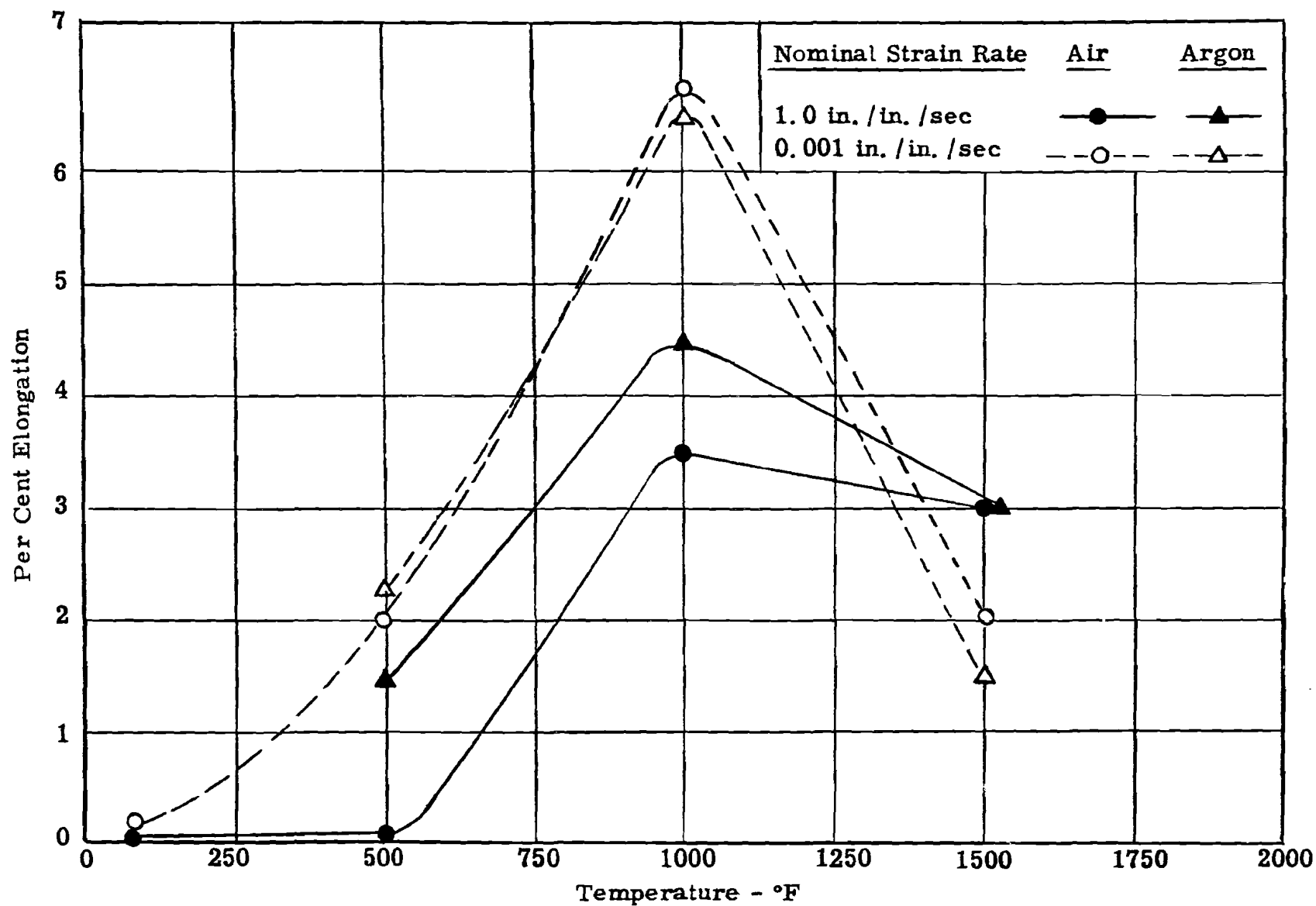
Figure 9. Effect of temperature on the percent elongation of unalloyed beryllium bar
at two strain rates in atmospheres of air and of argon.

slightly higher temperature, the values obtained at the higher strain rate apparently suffering greater losses at low temperatures than the values obtained at the slower strain rate. At room temperature and at both strain rates, all specimens except one failed before 0.2% offset was reached. A comparison of the elongation values in Figure 9 with the corresponding strength values in Figures 6 and 7 show that the low strength values are associated with low elongation values. These low strength values at low temperature are probably a result of the combination of the low ductility and the associated stress concentrations, and therefore, do not represent the inherent uniform strength of the beryllium. At temperatures from 500° F to 1500° F at the slower strain rate and from 1000° F to 1500° F at the faster strain rate, the reported strength data probably represent more closely the inherent properties of the beryllium because the ductility was somewhat higher at these temperatures than at the lower temperatures. More representative values of room-temperature strength could probably have been obtained at slower strain rates on specimens with smoother contours. At temperatures above 1000° F, the strength of the beryllium tended to increase with increasing strain rate, an effect which is normal in most metals. At lower temperatures, this inherent effect of strain rate was probably obscurred by the effect of the brittle fractures already discussed.

The scatter of the modulus-of-elasticity data as shown in Figure 8 is believed to be the result of the insufficient number of specimens for a better statistical evaluation and of the difficulty in determining the proper initial slope on the stress-strain curve rather than the result of any inherent effects of strain rate or of atmosphere.

In Figure 9 the percent elongation of beryllium increased at both strain rates with increasing temperature up to 1000° F and then decreased with further increasing temperature. At 1500° F, higher ductility was obtained at the higher strain rate but at all test temperatures below 1500° F, the slow strain rate produced the higher ductility. The erratic effects of variations in temperature and in strain rate on elongation values is characteristic of many metals.

No significant effects on any of the properties of beryllium are attributable to either of the two test atmospheres, air or argon. In the air atmosphere at all test temperatures up to and including 1500° F, no appreciable oxidation or discoloration of the beryllium specimens was observed. But if the supply of specimens had permitted testing up to 2000° F, the beneficial effect of the inert atmosphere would probably have become apparent.

SECTION IV. THE EVALUATION OF PROTECTIVE COATINGS

4.1 Purpose and Scope

Until the recent advent of atomic energy and missiles, the creation of new materials had kept pace with design requirements, but the critical environments of nuclear reactors and of space vehicles have brought about demands for super materials with properties exceeding those of any materials yet devised. While researchers dig into the fundamental structure of matter in order to develop the new super materials, engineers are seeking some sort of a compromise between the severe conditions and the known materials. One form of compromise is the composite material, in which two or more different types of material are joined in a composite structure to combine the desirable properties of each component. One component may be uniformly distributed within a matrix component, as cermets or plastic re-enforced with Fiberglas; or the components may be stratified, as sandwich constructions or surface coatings. From the latter category, nine combinations of base materials and surface coatings were evaluated to determine the short-time-tensile properties of the composite materials at elevated temperatures.

In the early missile-design considerations, the thermal, mechanical, or refractory properties of such materials as copper, nickel, graphite, molybdenum, and tantalum seemed to be attractive if the surfaces of these materials could be protected from chemical and mechanical erosion. In a previous study at Battelle Memorial Institute under Contract No. AF 33(616)-3227[1]; the effectiveness of the protection against erosion, oxidation, and thermal shock was determined for various coatings on copper, nickel, and graphite, and tantalum. On the basis of the findings of that study, some of the most promising combinations of base materials and coating materials were chosen for further evaluation in this program to determine the effect of the coatings on the short-time tensile properties of the base materials. The following combinations of base materials and coatings were evaluated: annealed ETP copper sheet with coatings of (1) electroplated chromium over nickel, (2) Rokide A (aluminum oxide), (3) Rokide Z (zirconium oxide) and (4) Rokide ZS (zirconium silicate); annealed A-nickel sheet with coating of

---

[1] Spraker, W. A.; Weeler, A. E.; Hess, R. E.; Harp, J. L.; and Bagby, F. L.; "The Development of Testing Procedures and the Evaluation of Coatings for Tantalum, Graphite, Nickel, and Copper," WADC TR 57-317, Wright Air Development Center, Wright-Patterson Air Force Base, Ohio

(5) chromium electroplate; arc-cast molybdenum sheet (as rolled at 1900° F to 2000° F) with a coating of (6) electroplated chromium over nickel; and type-GBH molded graphite with coatings of (7) Crystalon C (Si C), (8) Rokide Z (zirconium oxide), (9) Rokide ZS (zirconium silicate), and (10) silicon carbide-silicon nitride. In the tensile evaluations, the molded graphite was loaded in a direction perpendicular to the direction of the original forming pressure, and the sheet metals were loaded in the longitudinal direction.

The coatings were applied to machined tensile specimens as used in the previous phases of this work (shown in Figure 10). The metallic specimens were of sheet with a gage section of 2 in. long by 1/2 in. wide, and the graphite specimens were cylindrical with a gage section of 1 in. long by 3/8 in. diameter. The electroplated coatings on copper, nickel, and molybdenum were applied at Southern Research Institute. The thickness of each material in the plated coatings was 0.0015 to 0.0020 in. The Crystalon C, the Rokide A, the Rokide Z, and the Rokide ZS coatings were applied to the copper and the graphite specimens by proprietary processes at the Norton Company of Worchester Mass. The silicon carbide-silicon nitride coating was applied to graphite specimens by the National Carbon Company.

Among the materials evaluated during the original term of this contract were uncoated type—GBH graphite and sheet-type specimens of each of the same materials as those that were coated. The original plan was to evaluate the coated specimens with the same conditions of temperature, strain rate, and atmosphere that were used for the corresponding base material in its uncoated condition. However, some of the coatings could not tolerate temperatures as high as the temperatures used to evaluate the uncoated base material in an inert atmosphere. For these combinations, the test temperatures were lowered, until the coating remained intact, but often these lower temperatures were below the range of the available comparative data on the uncoated base materials. The coated specimens of metallic base were evaluated in both air and inert atmospheres; the coated specimens of graphite base were evaluated in air only.

4.2 Test Equipment and Procedure

The coated tensile specimens were evaluated with the basic test equipment already described in Section II of this report. The specimens were heated to test temperature within 30 sec and held at temperature for 90 sec before loading. The nominal strain rate was 0.001 in./in./sec. At least two specimens were used at each condition. On the copper specimens with coatings of Rokide A, Rokide Z, and Rokide ZS, the temperature of the specimen was measured with No. 36 chromel and alumel thermocouple wires

1/2 Size   Full Scale

Metallic Sheet-Type Specimen   Cylindrical Graphite Specimen
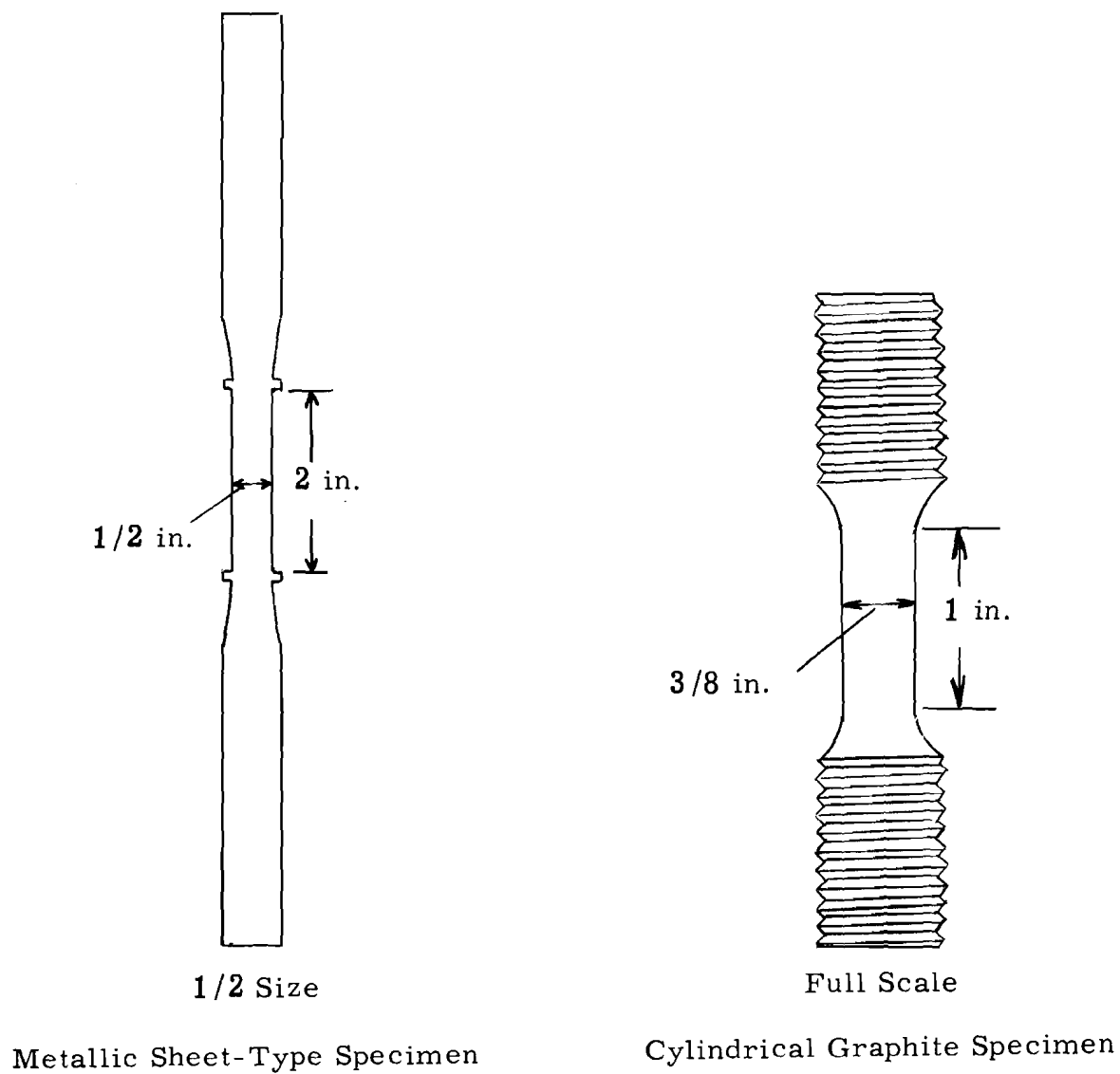
Figure 10. Tensile specimens to which coatings were applied.

welded to the surface of the copper specimen at the center of the gage section.
At a spot 1/16 in. in diameter, the coating was carefully ground away to
expose the copper surface. After the thermocouple was attached, the coating
was repaired around the couple with Sauereisen refractory cement. On the
copper, nickel, and molybdenum specimens with electroplated coatings, the
thermocouple wires were welded to the surface of the metallic coatings for
temperatures not exceeding 2500° F. At slightly more than 2500° F, on the
molybdenum specimens, the layers of chromium and nickel alloyed and
became fluid making temperature measurements very difficult. Above 2500° F
on the molybdenum specimens and on all graphite specimens, a total-radiation
pyrometer provided a signal to the temperature-control apparatus, and the
calibration of the control system was checked at each test temperature
against the indication of a Leeds and Northrup optical pyrometer.

Before the testing began on each type of coated material, the effect of
resistance heating on the integrity of the coating was determined. No detri-
mental effects on any of the coatings was observed as a result of resistance
heating at moderate to slow heating rates, but the Rokide coatings on graphite
were damaged by rapid resistance heating. The Rokide Z coating crazed,
and the Rokide ZS coating ballooned like an eggshell to about twice its
original diameter. It was desired to determine whether external heating
would produce any different effects. A battery of oxyacetylene torches were
tried for heating some of the graphite specimens with coatings of Rokide Z
and ZS, but it was impossible to distribute the flame sufficiently to obtain
anywhere near uniform temperature within the gage section. No significant
difference in the effect of temperature upon the coating could be observed
visually at the hot spots produced by the flames, so torch heating was not
used on any metallic specimens. Since a large effort would have been
required to construct a furnace capable of heating the graphite specimens to
3000° F, resistance heating with a slow heating rate was accepted as the
method for heating all coated specimens.

4.3 Results and Discussion

The tensile properties of the base materials were determined in the
earlier term of this contract, and, having been published in WADC TR 57-
649 Part I, these data will not be repeated in this report except graphically
for comparison with the similar properties of the coated specimens. For
each of the four metallic base materials, the solid lines without data points
on the graphs (Figure 11-20) show the various tensile properties of the
uncoated base materials as functions of test temperature. Then on the same
graphs, with a different symbol for each coating, the corresponding data
points are plotted for the coated specimens, but these data points are not →
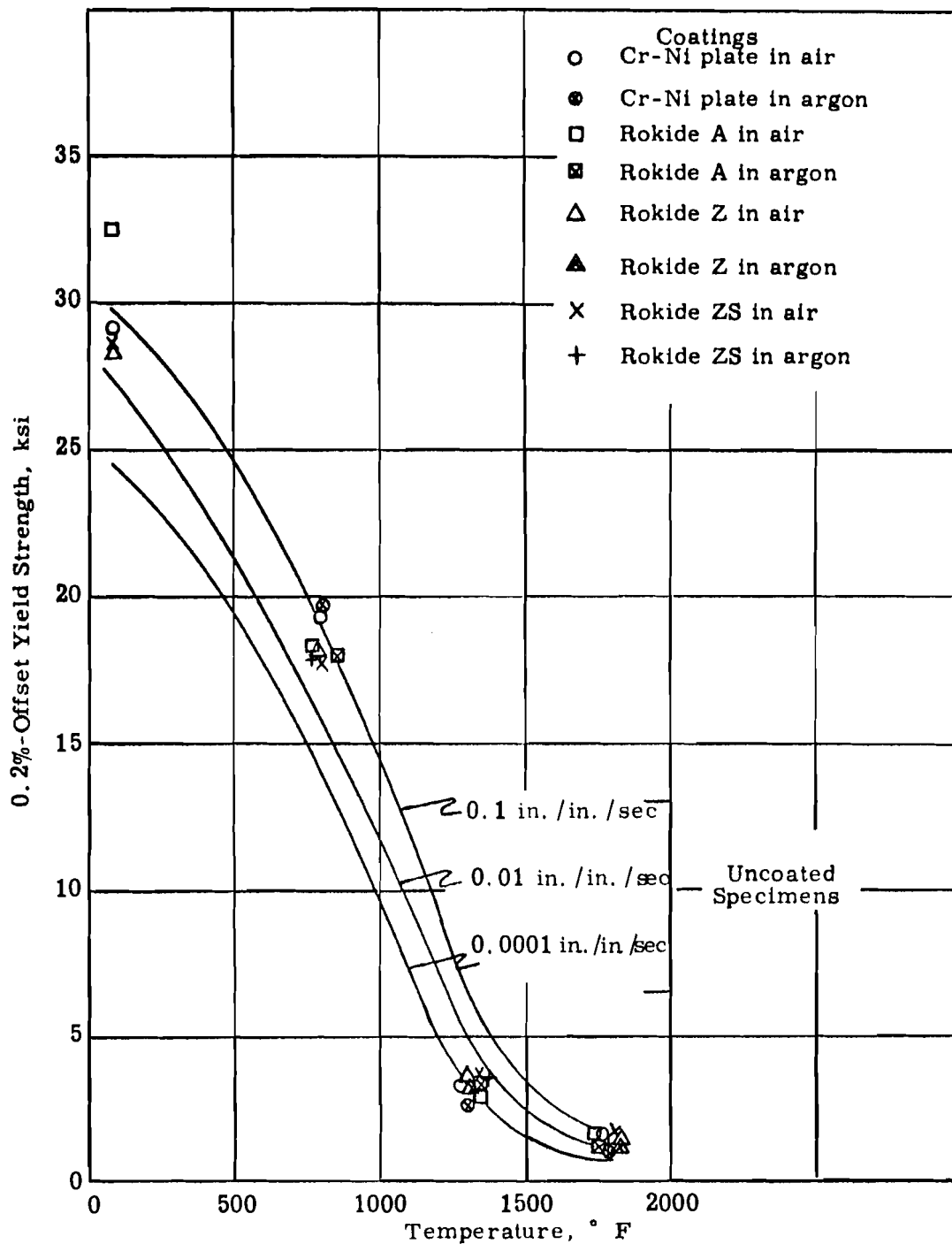
Figure 11. The effect of several protective coatings on the 0.2%-offset yield strength of annealed ETP copper sheet for a range of temperature from ambient to 1800° F. The coated specimens were tested at a nominal strain rate of 0.001 in. /in. /sec.
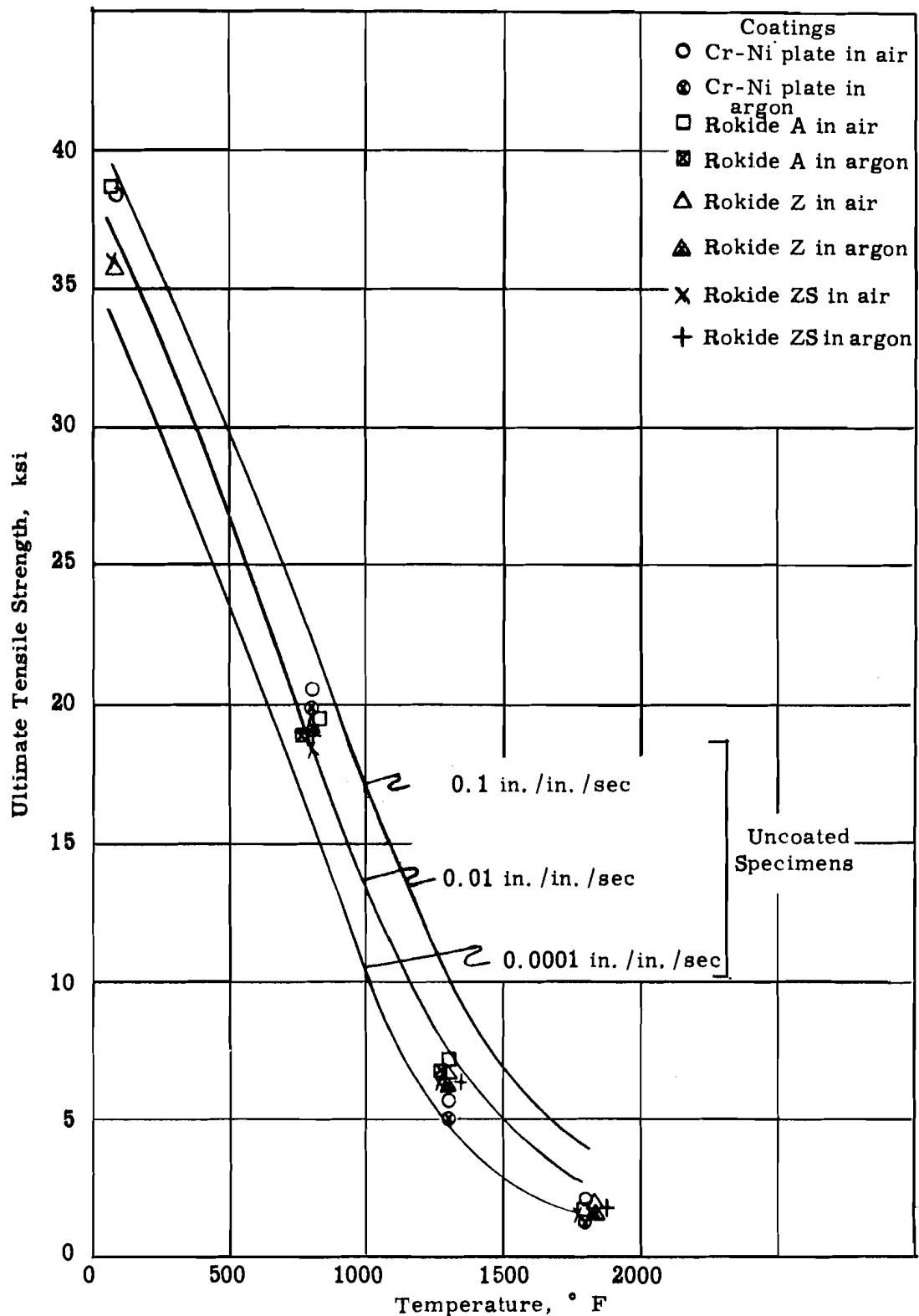
Figure 12. The effect of several protective coatings on the ultimate tensile strength of annealed ETP copper sheet for a range of temperature from ambient to 1800° F. The coated specimens were tested at a nominal strain rate of 0.001 in. /in. /sec.
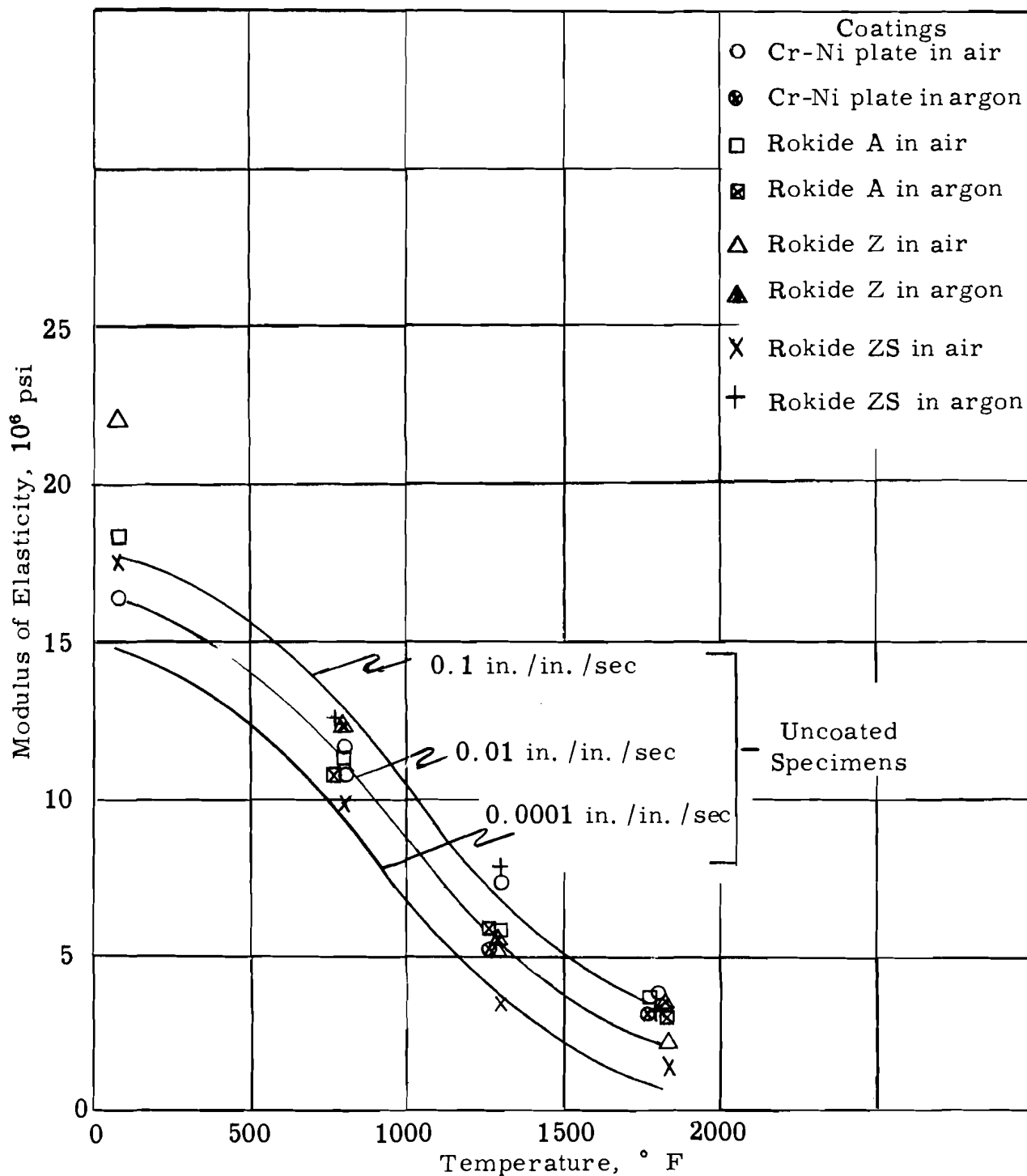
Figure 13. The effect of several protective coatings on the modulus of elasticity of annealed ETP copper sheet for a range of temperature from ambient to 1800° F. The coated specimens were tested at a nominal strain rate of 0.001 in. /in. /sec.
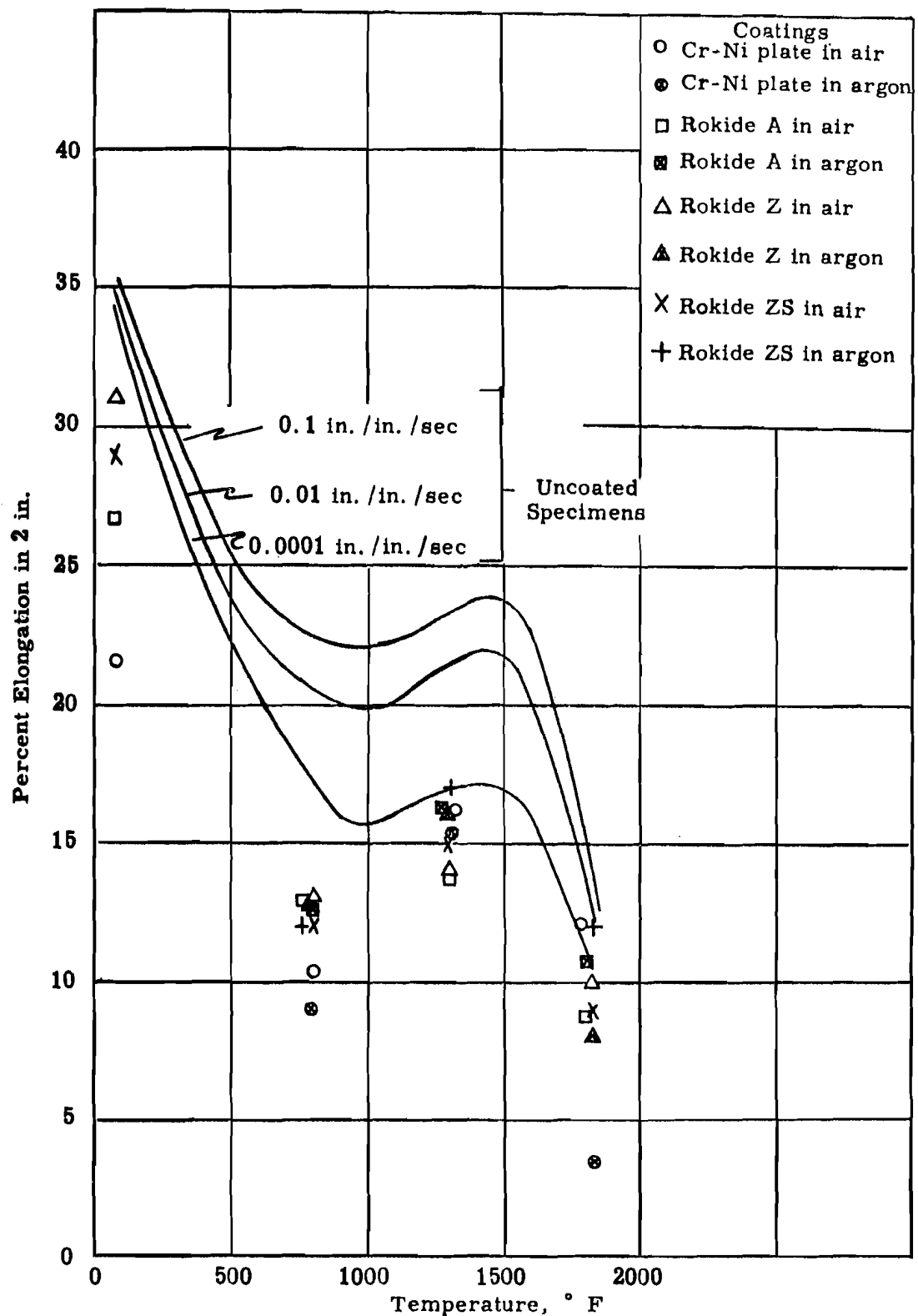
Figure 14. The effect of several protective coatings on the percent elongation of annealed ETP copper sheet for a range of temperature from ambient to 1800° F. The coated specimens were tested at a nominal strain rate of 0.001 in. /in. /sec.
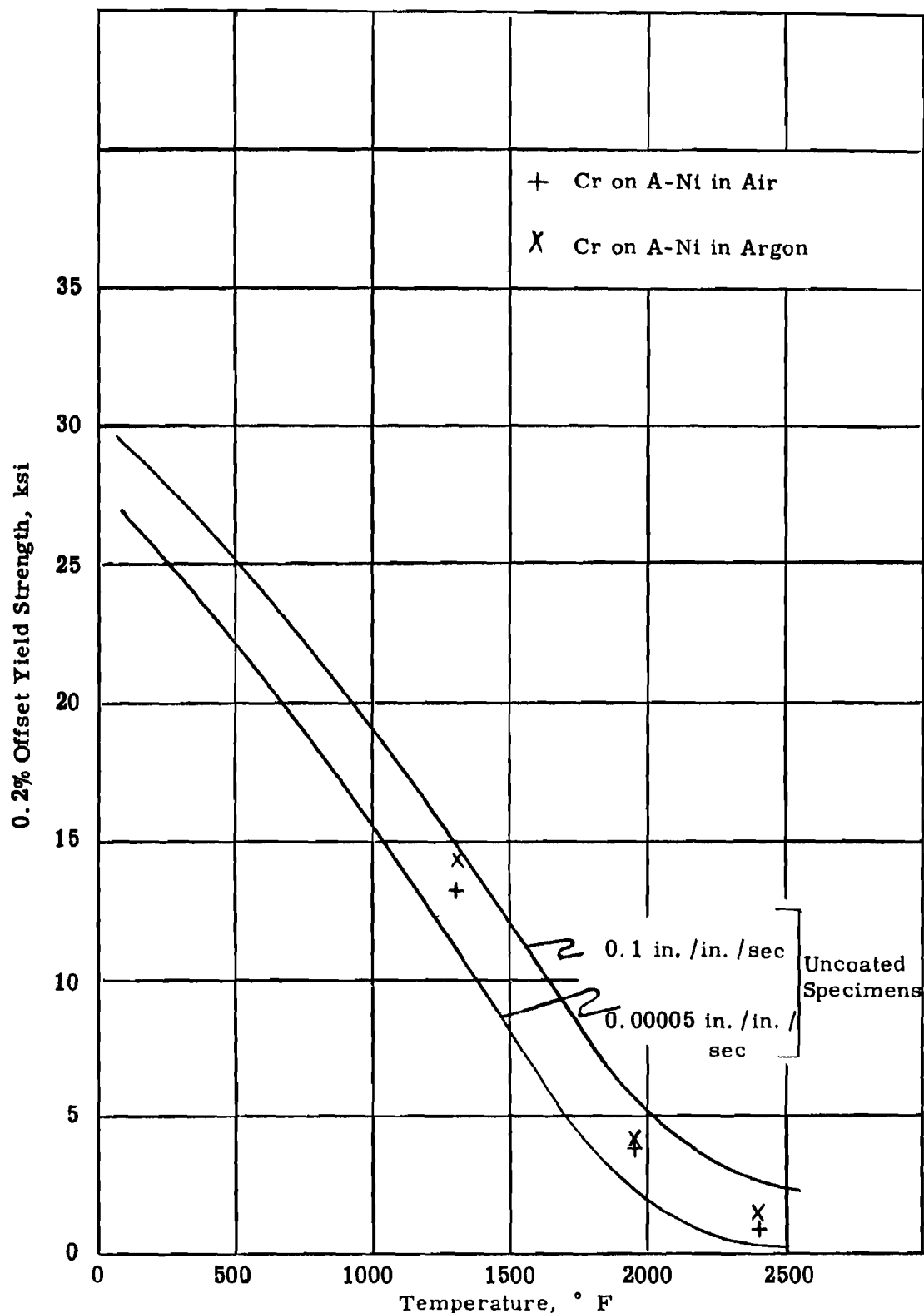
Figure 15. The effect of an electroplated coating of chromium on the 0.2%-offset yield strength of annealed A-nickel sheet for a range of temperature from ambient to 2500° F in air and argon. The coated specimens were tested at a nominal strain rate of 0.001 in./in./sec.
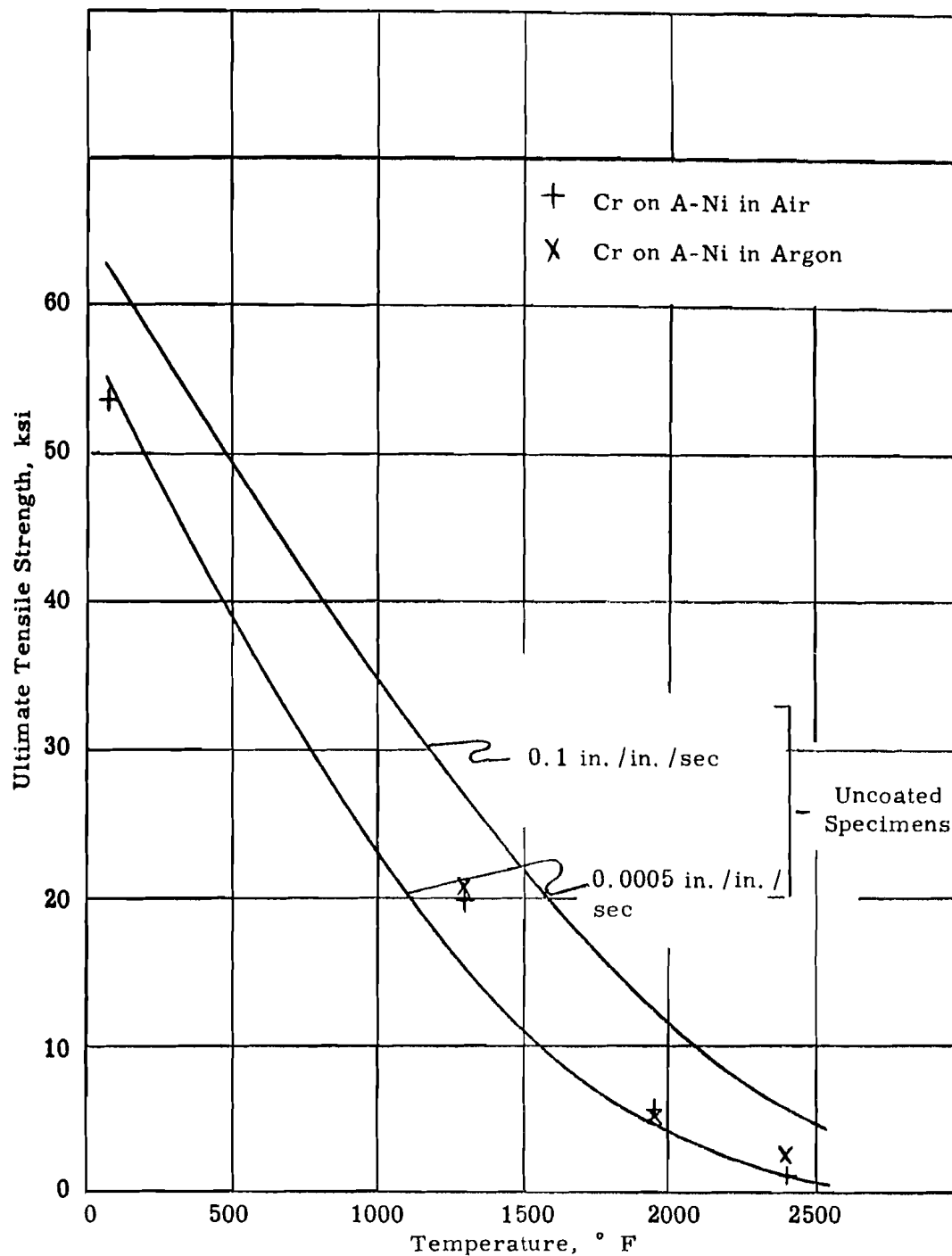
Figure 16. The effect of an electroplated coating of chromium on the ultimate tensile strength of annealed A-nickel sheet for a range of temperature from ambient to 2500° F in air and argon. The coated specimens were tested at a nominal strain rate of 0.001 in. /in. /sec.
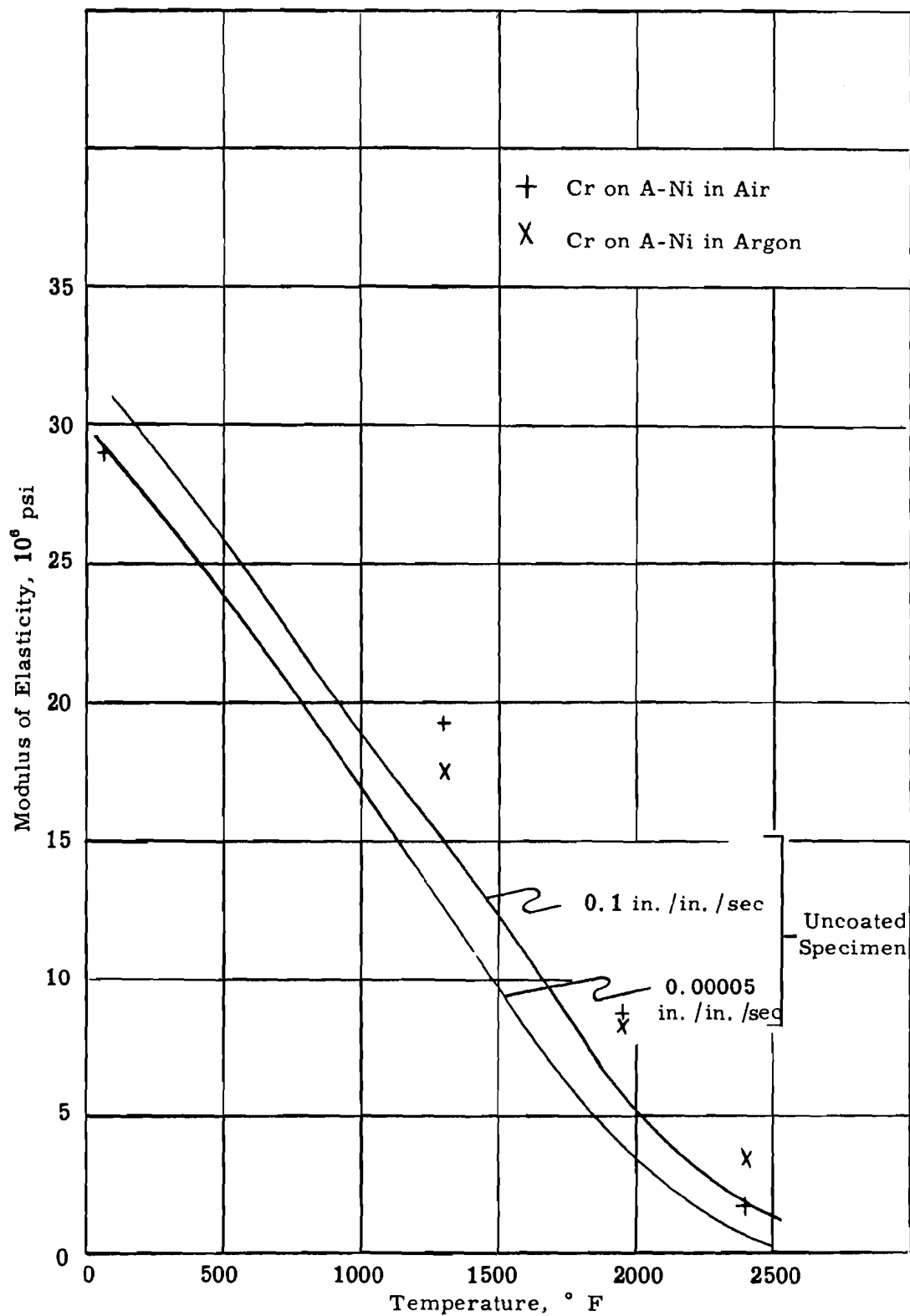
Figure 17. The effect of an electroplated coating of chromium on the
modulus of elasticity of annealed A-nickel sheet for a range
of temperature from ambient to 2500° F in air and argon.
The coated specimens were tested at a strain rate of 0.001
in./in./sec
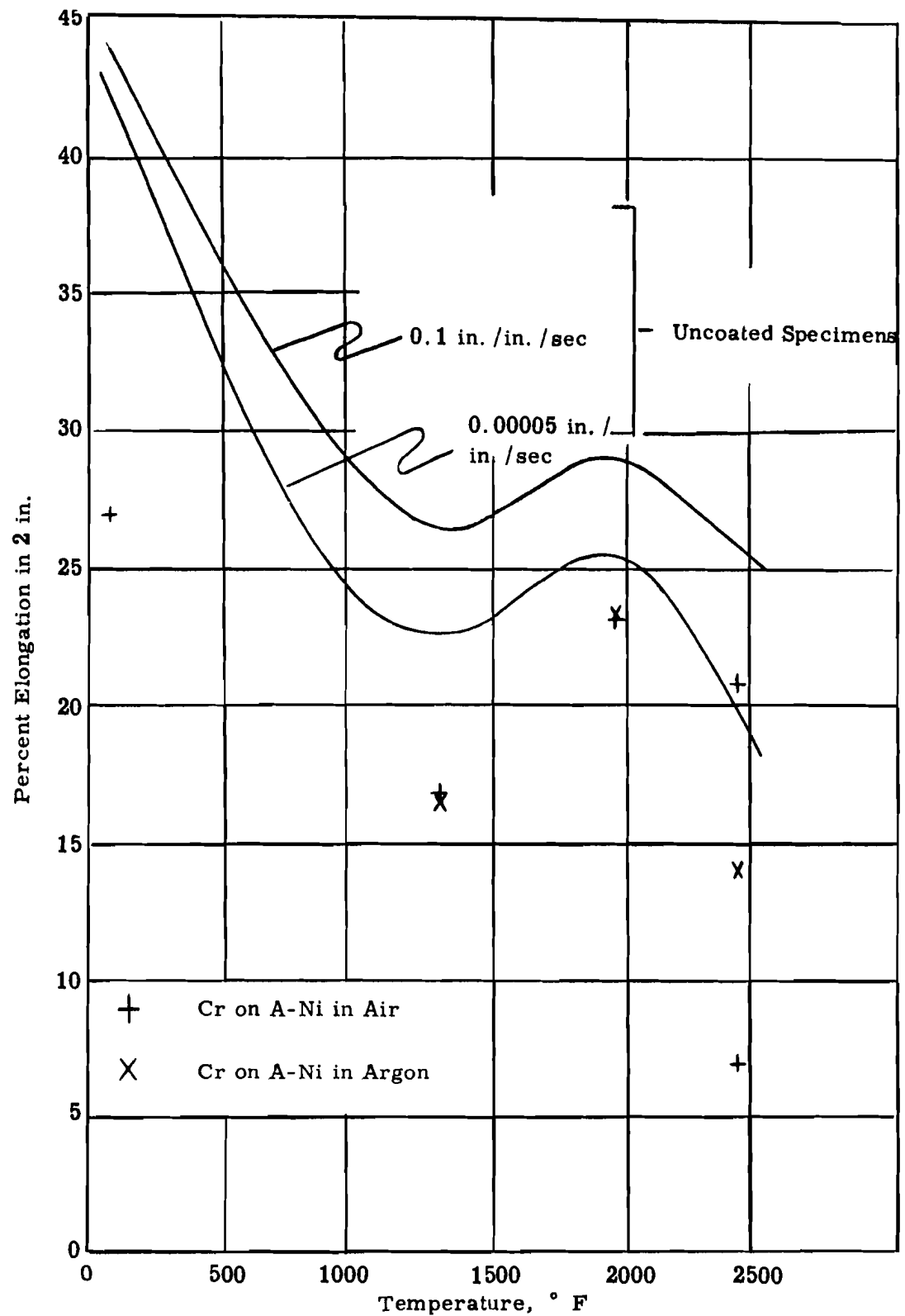
Figure 18. The effect of an electroplated coating of chromium on the percent elongation of annealed A-nickel sheet for a range of temperature from ambient to 2500° F in air and argon. The coated specimens were tested at a nominal strain rate of 0.001 in./in./sec.
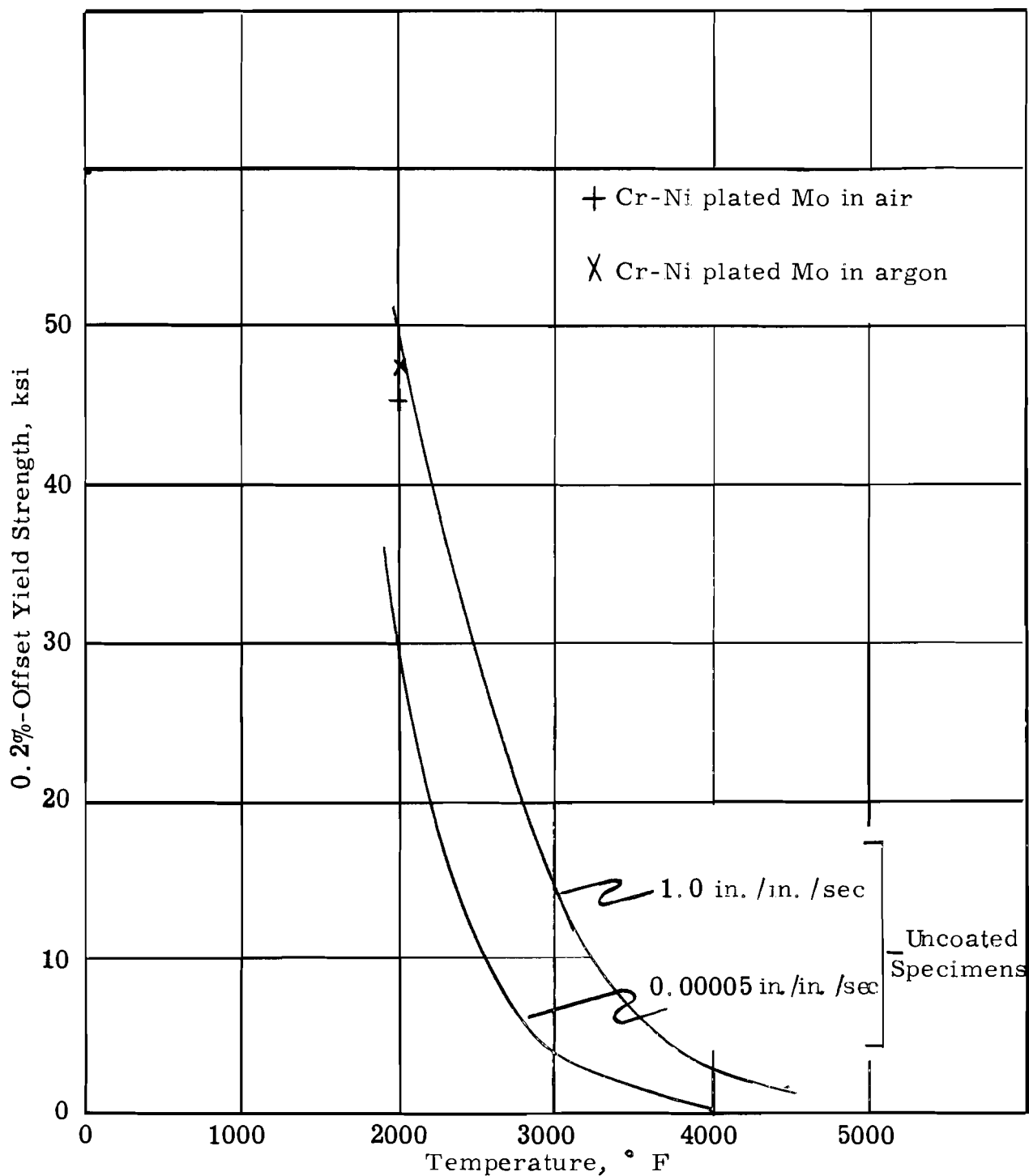
Figure 19.   The effect of an electroplated coating of chromium and nickel
on the 0. 2%-offset yield strength of arc-cast molybdenum
sheet at 2000° F in air and argon. The coated specimens
were tested at a nominal strain rate of 0. 001 in. /in. /sec.
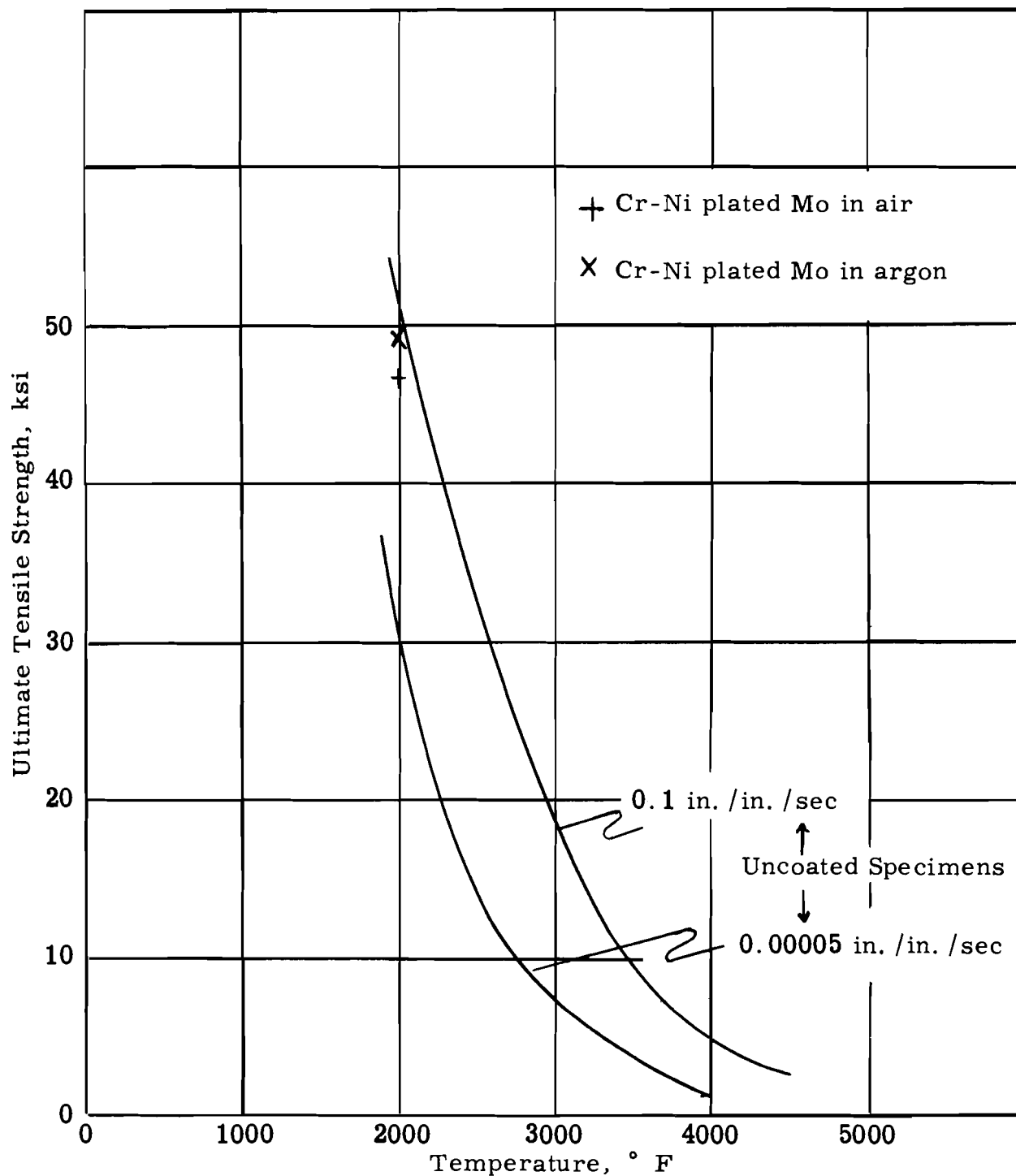
Figure 20. The effect of an electroplated coating of chromium and nickel on the ultimate tensile strength of arc-cast molybdenum sheet at 2000° F in air and argon. The coated specimens were tested at a nominal strain rate of 0.001 in./in./sec

connected with lines on the graphs because of the congestion that would result from the close correlation of most of the data. Figure 21 shows graphically the comparison between the tensile strength of uncoated type GBH graphite and the same type of graphite with four different protective coatings. Tables III through VIII show the complete results of the tensile-property determinations on all of the combinations of protective coatings on metallic specimens. Table IX presents similar results for all of the graphite specimens with various protective coatings. The cross section contributed by the metallic coatings was included in the calculation of stresses, but for the specimens with nonmetallic coatings, only the cross section of the base material was used to calculate the stress. The scatter of the strength data was generally greater for the coated specimens than for the uncoated specimens.

4.4 Conclusions

The tensile evaluations on the coated materials did not, in general, produce very revealing results. The small variations in the strength of the coated metallics were less than the difference between the measured strengths as based on the cross section of the uncoated material and as based on the cross section including the coating. Unless the load-bearing contribution of the coating itself is precisely known, the accuracy of the measurement is no better than this difference. So no significant effect was produced on either the 0.2%-offset yield strength, the ultimate tensile strength, or the modulus of elasticity by any of the coatings on any of the metallic base materials. The percent elongation within the 2 in. gage length was significantly lower for the coated metallic specimens compared with the elongation of the uncoated specimens of the same base metal. In each case, the coating was more brittle than the base metal, so the coating began to fail in a network of fine cracks at about the same time the ultimate load occurred. The cracks continued to enlarge with further straining. These cracks were sources of stress concentration, which probably caused most of the straining to be concentrated at the cracks, rather than to be uniformly distributed over the gage section, resulting in lower total elongation.

On the coated copper specimens, temperature alone up to the melting point of copper did not produce deterioration of any of the four coatings. The chromium electroplate on the nickel specimens was unharmed at all test temperatures including 2400° F. The chromium-nickel electroplate on the molybdenum specimens melted and alloyed at about 2500° F and was useful only up to 2000° F. Since the minimum temperature was 3000° F for the previous tests on uncoated molybdenum in an inert atmosphere, a few uncoated specimens were pulled at 2000° F in an inert atmosphere to provide at least the one comparison at 2000° F.

Table III

Tensile Properties of Annealed ETP Copper Sheet with an Electrodeposited Coating of Chromium and Nickel[1] at Different Temperatures in Atmospheres of Air and of Argon. All Specimens were Heated to Test Temperature within 20 Sec and Held 90 Sec Before Loading.

Temp °F	Atmosphere	Strain Rate in./in./sec	0.2%-Offset Yld. Str. 10^3 psi	Ultimate Tens. Str. 10^3 psi	Mod. Elast. 10^6 psi	% Elong. in 2 in.
RT	Air	0.0012	31.0	38.0	17.2	20.0
RT	Air	0.0014	27.9	38.8	15.6	21.5
RT	Air	0.0014	28.6	38.4	16.0	23.0
Avg			29.2	38.4	16.7	21.5
800	Air	0.0018	18.4	19.4	10.8	6.0
800	Air	0.0017	20.1	20.8	12.2	7.5
800	Air	0.0016	21.2	23.2	12.8	7.5
800	Air	0.0019	18.0	18.8	10.6	6.0
Avg			19.4	20.5	11.6	6.75
800	Argon	0.0014	19.3	19.6	9.8	8.3
800	Argon	0.0014	20.0	20.2	10.7	7.0
800	Argon	0.0014	19.5	19.9	12.0	7.0
Avg			19.6	19.9	10.8	7.4
1300	Air	0.0008	3.1	5.7	8.3	15.0
1300	Air	0.0018	3.4	6.0	7.0	17.0
1300	Air	0.0017	2.7	5.0	7.0	16.5
Avg			3.1	5.6	7.4	16.1

Table III (Cont'd)

Tensile Properties of Annealed ETP Copper Sheet with an Electrodeposited Coating of Chromium and Nickel[1] at Different Temperatures in Atmospheres of Air and of Argon. All Specimens were Heated to Test Temperature within 20 Sec and Held 90 Sec Before Loading.

Temp ° F	Atmosphere	Strain Rate in. /in. /sec	0.2%-Offset Yld. Str. 10^3 psi	Ultimate Tens. Str. 10^3 psi	Mod. Elast. 10^6 psi	% Elong. in 2 in.
1300	Argon	0.0021	2.7	4.5	4.9	20.0
1300	Argon	0.0023	2.7	5.8	4.8	16.5
1300	Argon	0.0025	2.5	4.7	5.5	9.0
Avg			2.6	5.0	5.1	15.1
1800	Air	0.0016	1.6	2.1	3.9	14.0
1800	Air	0.0017	1.4	1.7	4.0	2.5
1800	Air	0.0016	1.5	1.7	2.9	12.0
1800	Air	0.0019	1.6	1.9	3.2	10.0
Avg			1.5	1.8	3.6	9.6
1800	Argon	0.0017	1.1	1.3	3.0	3.5
1800	Argon	0.0020	0.9	1.1	3.4	2.5
1800	Argon	0.0020	1.1	1.4	3.1	4.0
			1.0	1.3	3.2	3.3

[1] Chromium was plated over nickel, each layer being 0.0015 to 0.0020 in. thick.

Table IV

Tensile Properties of Annealed ETP Copper Sheet with a Protective Coating
of Rokide A[1] at Different Temperatures in Atmospheres of Air and Argon.
All Specimens were Heated to Test Temperature Within 20 Sec and Held
90 Sec Before Loading.

Temp. ° F	Atmosphere	Strain Rate in./in./sec	0.2%-Offset Yld. Str. 10^3 psi	Ultimate Tens. Str. 10^3 psi	Mod. Elast. 10^6 psi	% Elong. in 2 in.	Notes
RT	Air	0.0009	33.0	38.3	19.2	27.5	2
RT	Air	0.0010	33.0	37.2	17.8	26.5	2
RT	Air	0.0015	30.4	38.3	17.9	26.5	2
RT	Air	0.0015	33.6	40.0	18.3	26.0	2
Avg			32.5	38.5	18.3	26.5	
800	Air	0.0017	18.1	19.1	11.0	12.5	3
800	Air	0.0017	18.2	20.0	11.5	13.0	3
Avg			18.2	19.6	11.3	12.7	3
800	Argon	0.0018	17.9	19.2	10.2	14.0	
800	Argon	0.0019	18.6	19.3	11.8	12.0	
800	Argon	0.0014	17.4	18.3	9.6	11.5	
Avg			18.0	18.9	10.6	12.5	
1300	Air	0.0020	4.0	7.2	7.4	14.5	3
1300	Air	0.0020	3.8	7.4	4.9	14.0	3
1300	Air	0.0020	3.7	6.8	3.0	14.0	3
1300	Air	0.0020	3.4	7.1	6.8	12.5	
Avg			3.8	7.1	5.5	13.7	
1300	Argon	0.0020	3.8	6.7	3.6	16.5	
1300	Argon	0.0018	3.4	6.3	5.9	15.0	
1300	Argon	0.0016	3.4	6.7	8.1	17.0	
Avg			3.5	6.6	5.9	16.1	

Table IV (Cont'd)

Tensile Properties of Annealed ETP Copper Sheet with a Protective Coating
of Rokide A[1] at Different Temperatures in Atmospheres of Air and Argon.
All Specimens were Heated to Test Temperature Within 20 Sec and Held
90 Sec Before Loading.

Temp ° F	Atmosphere	Strain Rate in. /in. /sec	0. 2%-Offset Yld. Str. 10^3 psi	Ultimate Tens. Str. 10^3 psi	Mod. Elast. 10^6 psi	% Elong. in 2 in.	Notes
1825	Air	0.0020	1.7	1.9	4.7	11.0	
1825	Air	0.0020	1.7	1.8	2.4	7.5	
Avg			1.7	1.8	3.5	9.3	
1825	Argon	0.002	1.2	1.5	4.5	8.0	
1825	Argon	0.002	1.3	1.9	2.7	13.0	
1825	Argon	0.002	1.3	1.7	3.1	11.0	
Avg			1.3	1.7	3.4	10.6	

Notes: 1. Aluminum oxide applied by Norton Company.

2. Coating cracked off soon after start of loading.

3. Coating cracked at start of loading but did not come off until fracture.

Table V

Tensile Properties of Annealed ETP Copper Sheet with a Protective Coating
of Rokide Z[1] at Different Temperatures in Atmospheres of Air and Argon.
All Specimens were Heated to Test Temperature Within 20 Sec and Held
90 Sec Before Loading.

Temp. ° F	Atmosphere	Strain Rate in./in./sec	0.2%-Offset Yld. Str. 10^3 psi	Ultimate Tens. Str. 10₃ psi	Mod. Elast. 10^6 psi	% Elong. in 2 in.
RT	Air	0.0011	28.6	35.1	18.1	32.5
RT	Air	0.0011	30.7	36.0	16.6	30.0
Avg			29.7	35.6	17.4	31.3
800	Air	0.00095	16.8	18.3	11.6	12.5
800	Air	0.00094	17.4	18.8	13.8	11.5
Avg			17.1	18.6	12.7	12.0
800	Argon	0.0011	18.5	19.4	11.8	13.5
800	Argon	0.0013	18.0	18.7	12.8	12.5
Avg			18.3	19.1	12.3	13.0
1300	Air	0.0017	3.38	6.55	5.7	14.0
1300	Air	0.0017	2.74	6.05	4.9	15.0
1300	Air	0.0013	3.64	6.92	5.9	13.5
Avg			3.25	6.51	5.5	14.2
1300	Argon	0.0011	3.57	6.33	5.4	16.5
1300	Argon	0.0014	3.44	6.40	6.2	15.0
Avg			3.51	6.37	5.8	15.8
1825	Air	0.0011	1.51	1.82	2.0	10.0
1825	Air	0.0021	1.53	1.99	1.1	10.0
1825	Air	0.0014	1.60	1.82	2.1	10.0
Avg			1.55	1.88	1.7	10.0

Table V (Cont'd)

Tensile Properties of Annealed ETP Copper Sheet with a Protective Coating of Rokide Z[1] at Different Temperatures in Atmospheres of Air and Argon. All Specimens were Heated to Test Temperature Within 20 Sec and Held 90 Sec Before Loading.

Temp. ° F	Atmosphere	Strain Rate in. /in. /sec	0. 2%-Offset Yld. Str. 10^3 psi	Ultimate Tens. Str. 10^3 psi	Mod. Elast. 10^6 psi	% Elong. in 2 in.
1825	Argon	0.0010	1.26	1.66	3.6	7.5
1825	Argon	0.0014	1.35	1.66	3.1	7.5
Avg			1.31	1.66	3.4	7.5

1. Zirconium oxide applied by Norton Co.

Table VI

Tensile Properties of Annealed ETP Copper Sheet with a Protective Coating
of Rokide ZS[1] at Different Temperatures in Atmospheres of Air and Argon.
All Specimens were Heated to Test Temperature Within 20 Sec and Held
90 Sec Before Loading.

Temp. ° F	Atmosphere	Strain Rate in./in./sec	0.2%-Offset Yld. Str. 10^3 psi	Ultimate Tens. Str. 10^3 psi	Mod. Elast. 10^6 psi	% Elong. in 2 in.
RT	Air	0.0012	28.5	31.3	17.0	27.5
RT	Air	0.0012	28.8	34.0	16.9	30.5
Avg			28.7	32.7	17.0	29.0
800	Air	0.0015	16.8	18.1	10.6	11.5
800	Air	0.0017	17.7	18.6	9.2	11.5
Avg			17.3	18.4	9.9	11.5
800	Argon	0.0015	17.5	18.5	12.8	12.0
800	Argon	0.0014	18.0	19.0	13.5	11.5
Avg			17.8	18.8	13.2	11.8
1300	Air	0.0013	3.46	6.25	4.4	14.0
1300	Air	0.0014	3.38	6.60	3.7	15.0
1300	Air	0.0012	3.69	6.47	7.1	13.0
Avg			3.51	6.44	5.1	14.0
1300	Argon	0.0013	3.69	6.34	7.21	17.0
1300	Argon	0.0011	3.69	6.15	7.87	16.5
Avg			3.69	6.25	7.54	16.8

Table VI (Cont'd)

Tensile Properties of Annealed ETP Copper Sheet with a Protective Coating
of Rokide ZS[1] at Different Temperatures in Atmospheres of Air and Argon.
All Specimens were Heated to Test Temperature Within 20 Sec and Held
90 Sec Before Loading.

Temp. ° F	Atmosphere	Strain Rate in./in./sec	0.2%-Offset Yld. Str. 10^3 psi	Ultimate Tens. Str. 10^3 psi	Mod. Elast. 10^6 psi	% Elong. in 2 in.
1825	Air	0.0015	1.47	1.74	1.2	13.0
1825	Air	0.0012	1.45	1.58	1.8	5.5
1825	Air	0.0012	1.52	1.65	1.8	8.5
Avg			1.48	1.66	1.6	9.0
1825	Argon	0.0008	1.32	1.65	3.0	11.0
1825	Argon	0.0012	1.28	1.59	3.7	14.0
Avg			1.30	1.62	3.4	12.5

[1] Zirconium silicate applied by Norton Company.

Table VII

Tensile Properties of Annealed A-Nickel Sheet with an Electrodeposited Coating of Chromium[1] at Different Temperatures in Atmospheres of Air and Argon. All Specimens were Heated to Test Temperature Within 20 Sec and Held 90 Sec Before Loading.

Temp. ° F	Atmosphere	Strain Rate in./in./sec	0.2%-Offset Yld. Str. 10^3 psi	Ultimate Tens. Str. 10^3 psi	Mod. Elast. 10^6 psi	% Elong. in 2 in.
RT	Air	0.0008	28.1	54.0	27.0	23.5
RT	Air	0.0010	28.3	54.9	29.7	29.0
RT	Air	0.0010	24.4	52.0	29.6	28.5
Avg			26.9	53.4	28.8	27.0
1300	Air	0.0016	12.6	18.9	29.9	17.0
1300	Air	0.0013	12.3	21.9	29.9	17.5
1300	Air	0.0014	12.1	17.7	23.0	16.0
1300	Air	0.0018	13.8	20.6	20.7	16.5
Avg			12.7	19.8	25.8	16.7
1300	Argon	0.0014	15.2	21.0	--	19.5
1300	Argon	0.0014	--	19.4	12.8	17.0
1300	Argon	0.0017	14.7	20.3	17.8	16.5
1300	Argon	0.0020	13.6	20.8	16.4	15.0
1300	Argon	0.0020	13.7	20.7	--	16.5
1300	Argon	0.0020	15.0	21.5	17.3	15.5
Avg			14.4	20.6	16.1	16.6
1950	Air	0.0020	3.5	5.9	8.3	22.5
1950	Air	0.0020	4.1	6.0	12.5	25.0
1950	Air	0.0020	3.8	5.6	8.7	21.0
1950	Air	0.0020	3.7	5.2	9.5	24.0
Avg			3.7	5.6	9.8	23.1

Table VII (Cont'd)

Tensile Properties of Annealed A-Nickel Sheet with an Electrodeposited Coating of Chromium[1] at Different Temperatures in Atmospheres of Air and Argon. All Specimens were Heated to Test Temperature Within 20 Sec and Held 90 Sec Before Loading.

Temp. ° F	Atmosphere	Strain Rate in. /in. /sec	0.2%-Offset Yld. Str. 10^3 psi	Ultimate Tens. Str. 10^3 psi	Mod. Elast. 10^6 psi	% Elong. in 2 in.
1950	Argon	0.0026	4.3	5.3	10.4	20.5
1950	Argon	0.0021	3.6	5.7	8.5	27.0
1950	Argon	0.0018	3.9	5.7	10.9	22.5
Avg			3.9	5.6	9.9	23.3
2400	Air	0.0020	0.9	1.3	1.7	7.0
2400	Air	0.0020	0.8	1.0	1.7	6.5
2400	Air	0.0020	0.7	1.1	—	7.5
2400	Air	0.0020	0.7	1.0	1.1	7.0
Avg			0.8	1.1	1.5	7.0
2400	Argon	0.0020	1.1	1.9	6.0	17.5
2400	Argon	0.0020	1.2	2.0	6.0	21.0
2400	Argon	0.0020	1.2	1.9	4.0	23.5
2400	Argon	0.0019	1.4	2.3	6.3	—
2400	Argon	0.0030	1.5	2.1	10.5	11.0
Avg			1.3	2.0	6.5	18.3

[1] Thickness of Cr deposit was 0.0015 to 0.0020 in.

Table VIII

Tensile Properties of Arc-Cast Molybdenum Sheet with an Electrodeposited Coating of Chromium and Nickel[1] at Different Temperatures in Atmospheres of Air and Argon. All Specimens were Heated to Test Temperature Within 20 Sec and Held 90 Sec Before Loading.

Temp. ° F	Atmosphere	Strain Rate in. /in. /sec	0.2%-Offset Yld. Str. 10^3 psi	Ultimate Tens. Str. 10^3 psi	Mod. Elast. 10^6 psi	% Elong. in 2 in.	Notes
2000	Air	0.0015	44.6	46.8	26.2	6.0	
2000	Argon	0.0012	45.1	46.2	–	6.0	
2000	Argon	0.0015	46.6	48.1	25.6	6.0	
2000	Argon	0.0015	45.1	47.0	25.2	6.0	
Avg			45.6	47.1	25.4	6.0	
2400	Air	0.0017	8.6	12.6	25.0	2.0	
2450	Air	0.0018	7.2	9.0	24.6	1.5	
2500	Air	0.0013	8.1	9.8	26.0	3.0	
2500	Air	0.0019	7.3	8.2	–	2.5	
Avg			7.7	9.0	26.0	2.8	
2500	Argon	0.0008	7.1	7.3	22.7	2.0	
3000	Argon	–	4.3	4.3	13.0	<1	
2000	Air	0.0015	45.9	46.5	25.7	8.0	2

Table VIII (Cont'd)

Tensile Properties of Arc-Cast Molybdenum Sheet with an Electrodeposited Coating of Chromium and Nickel[1] at Different Temperatures in Atmospheres of Air and Argon. All Specimens were Heated to Test Temperature Within 20 Sec and Held 90 Sec Before Loading.

Temp. ° F	Atmosphere	Strain Rate in. /in. /sec	0. 2%-Offset Yld. Str. 10^3 psi	Ultimate Tens. Str. 10^3 psi	Mod. Elast. 10^6 psi	% Elong. in 2 in.	Notes
2000	Argon	0.0015	48.7	50.1	27.5	6.5	2
2000	Argon	0.0013	50.5	51.6	31.9	8.5	2
2000	Argon	0.0016	45.4	46.0	28.5	5.0	2
Avg			46.2	49.6	29.3	6.6	

[1] Chromium was plated over nickel, each layer being 0.0015 to 0.0020 in. thick.

[2] Uncoated molybdenum run for comparison since the minimum test temperature was 3000° F for the previous tests on uncoated molybdenum.

Table IX.

Tensile Strength of GBH Graphite with Various Surface Coatings at Different Temperatures in Air. Nominal Strain Rate was 0.0001 in./in./sec. All Specimens were Heated to Temperature in 2 to 5 Min.

Type of Coating	Heat Source	Temp. ° F	Time at Temp. Sec	Tensile Strength psi	Remarks⁵
Crystalon C²	—	RT	—	1855	
Crystalon C²	—	RT	—	1840	
Crystalon C²	—	RT	—	1980	Irradiated (1)
Crystalon C²	Resistance	2500	180	2020	
Crystalon C²	Resistance	3600	30		
Crystalon C²	Oxyacetylene	3300	60		
Crystalon C²	Oxyacetylene	3300	99	2460	
Rokide Z³	—	RT	—	2090	
Rokide Z³	—	RT	—	2230	
Rokide Z³	—	RT	—	2660	
Rokide Z³	Oxyacetylene	2700	10	3180	Broke outside gage
Rokide Z³	Oxyacetylene	2700	10	3040	Irradiated (1)
Rokide Z³	Oxyacetylene	2700	54	3240	Irradiated (1)
Rokide Z³	Oxyacetylene	3000	10	3230	
Rokide Z³	Oxyacetylene	3500	10	2680	
Rokide ZS⁴	—	RT	—	2330	
Rokide ZS⁴	—	RT	—	2710	
Rokide ZS⁴	—	RT	—	3210	
Rokide ZS⁴	—	RT	—	2490	Irradiated (1)
Rokide ZS⁴	—	RT	—	2760	Irradiated (1)
Rokide ZS⁴	Oxyacetylene	2700	45	3720	
Rokide ZS⁴	Oxyacetylene	2700	30	3670	
Rokide ZS⁴	Oxyacetylene	2700	114	3220	Broke outside gage

Table IX (Cont'd)

Tensile Strength of GBH Graphite with Various Surface Coatings at Different Temperatures in Air.   Nominal Strain Rate was 0.0001 in. /in. /sec.   All Specimens were Heated to Temperature in 2 to 5 Min.

Type of Coating	Heat Source	Temp. ° F	Time at Temp. Sec	Tensile Strength psi	Remarks[5]
SiC-SiN	Resistance	2500	30	1910	
SiC-SiN	Resistance	3000	30	2550	
SiC-SiN	Resistance	3000	240	1910	
SiC-SiN	Resistance	3200	150	1840	
SiC-SiN	Resistance	3200	30	2230	Overheated on heat-up

[1] Received a total irradiation of 1.17×10^7 roentgens from cobalt-60 source.

[2] Silicon carbide

[3] Zirconium oxide

[4] Zirconium silicate

[5] % Elongation was zero on all specimens

None of the coatings that were evaluated on type GBH graphite enhanced its short-time tensile properties—shown graphically in Figure 21—but all four of the coatings did provide good long-time protection from oxidation at temperatures up to 2600° F. The adhesion and the protection were superior for the Crystalon C and for the SiC-SiN coatings up to about 3200° F, which is the maximum temperature that these coatings can withstand for short-time applications of two minutes and less. These two coatings, which are applied by chemical reaction with the surface of the graphite body, appeared to materially reduce the strength of the graphite body. The two types of Rokide coatings, which were applied by a flame-spraying technique, are held in place by a mechanical interlocking of the coating particles with little bonding to the base material. The thermal expansion of the base material and the temperature gradient across the coating material both contributed to early failure of the coating. For short-time applications of two minutes and less, an apparent maximum operating temperature of 2700° F without coating failure was observed for the graphite tensile specimens with coatings of Rokide Z and Rokide ZS. Since the melting temperature for the Rokide Z is 4500° F and for the Rokide ZS is 3000° F, operating temperatures higher than 2700° F might be expected and, indeed, might be observed under more favorable conditions of thermal stress on the coating. An example of a more favorable application would be on the inside of a rocket nozzle, where the coating would be in compression.

In such an evaluation program to determine short-time tensile properties at elevated temperatures, about the only contribution that could be expected from a surface coating would be some degree of protection from oxidation in still air. Since neither copper nor nickel suffer rapid oxidation for short exposures to elevated temperatures, it is to be expected that little improvement in the mechanical properties would result from the application of coatings to these materials. On molybdenum and graphite, the coatings did prevent oxidation during exposure to elevated temperature within the range of temperatures that the coatings themselves could withstand. But coatings have not yet been devised to give adequate protection up to the maximum temperatures that molybdenum or graphite could be structurally serviceable. The evaluation under Contract No. AF 33(616)-3227 (referred to in Section 4.1) probably measured the more significant contributions of the coatings in determining the effectiveness of protection against erosion, oxidation, and thermal shock.
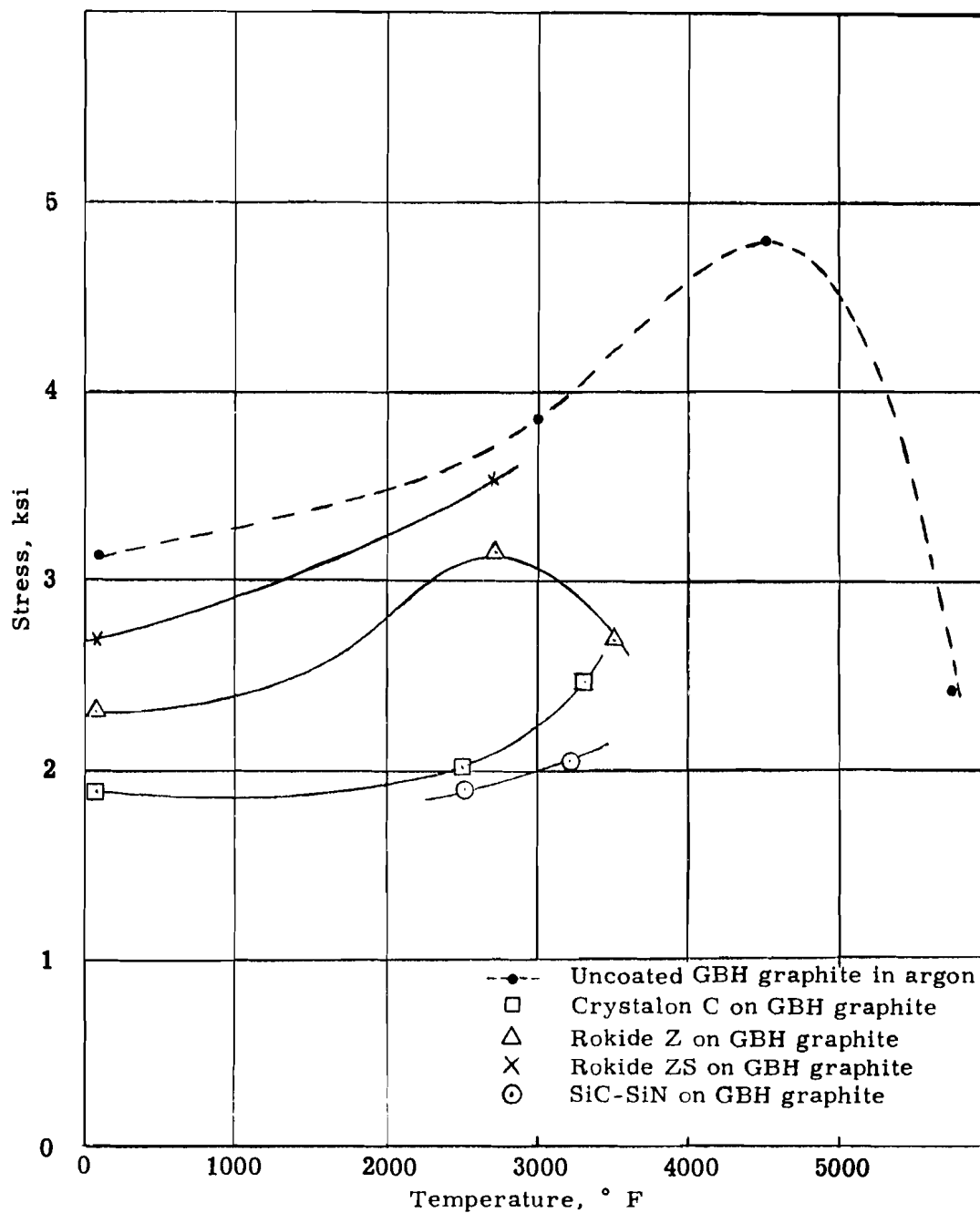
Figure 21. The effect of several protective coatings on the short-time
tensile strength of type GBH graphite over the useful range
of temperature. The uncoated graphite was tested in a
protective atmosphere of argon, but the coated samples of
the same graphite were tested in air.

SECTION V. EFFECTS ON TENSILE PROPERTIES PRODUCED BY THERMAL GRADIENTS TRANSVERSE TO THE AXIS OF LOADING

5.1 Purpose and Scope

The purpose of this phase of the work was twofold—(1) to measure by suitable test methods the tensile properties of a typical aircraft-structural alloy in the presence of transverse thermal gradients with magnitudes as large as practical and (2) to compare these measured properties with the same properties calculated for the same conditions by whatever analytical methods that are being used currently by structural designers of the major aircraft and missile manufacturers.

5.2 Design-Procedure Survey

Before the experimental work with thermal gradients was started, a survey was made among the structural designers of most of the major manufacturers of aircraft and missiles. A letter, reproduced in Figure 22, was sent to 31 companies to solicit their comments on their method of attack on structural design problems involving thermal gradients. A complete list of the respondents is given in Table X. A variety of comments was found in the eighteen replies received. Some of the replies indicated no difficulty with thermal gradients in thin skins because, in general, the gradients were negligible. Some wrote that a thermal gradient of 5000° F/in. (the figure mentioned in the letter) was too large and that a more reasonable thermal gradient for test purposes would be 1000° F/in. The opinion was expressed by a few that tensile properties of specimens subjected to thermal gradients would not be of any more value than regular high-temperature tests. Several companies indicated considerable interest in the problem of thermal gradients and expressed a desire for the test work to be conducted.

Contained in several of the replies were general descriptions of methods for the calculation of thermal stresses set up in a specimen due to a thermal gradient. Table XI lists most of these methods as well as several methods for calculating ultimate strength when thermal stresses are present. Since most of the discussions were only of a general nature, numerical results could be obtained with only one (discussed later in the report) of the methods listed in the table. Most of these methods were variations of the classical elastic theory. In some cases, the specimen was divided into laminae. The material properties at the average temperature of each lamina were used to calculate the thermal stresses. In other cases, mean values or empirical procedures were used to calculate thermal stresses.

Gentlemen:

As you know, for the past few years, we have been investigating for the Air Force the high-temperature properties of metals under conditions of rapid heating and rapid loading. I would like to ask for your help in our gathering of information for a new phase of this work, which we are now undertaking.

Although structural components in missiles and aircraft are sometimes subjected to simultaneous loads and thermal gradients, very little experimental data are available on the properties of metals with thermal gradients. Therefore, we are planning to determine the tensile properties of a number of sheet metals while they are subjected to a temperature gradient of about 5000° F per inch through the thickness of the specimens.

In order to orient ourselves for this work we are, at the suggestion of the Air Force, conducting a survey to determine design methods and experimental methods that are now in use or are available for solving design problems that involve thermal gradients. Would you give us the benefit of your experience on how such problems are handled in the aircraft or missile industries? If this question is outside your sphere of interest, would you please pass the letter along to someone else in your company who is qualified to answer.

I realize that a complete and comprehensive answer to this question may require more time than you can spare, but I would appreciate receiving just a general answer that points out the approaches that are taken but not mathematical details. Also, any literature references that you can give me on the subject would be very helpful.

Your comments would certainly be a great help to us in planning our work. May I hear from you at your earliest convenience, as the Air Force wants us to initiate our testing work as soon as possible.

Sincerely,

J. R. Kattus, Head
Metallurgy Division

jrk dpb
756　　　　　　　　Figure 22. Reproduction of survey letter.

Table X

Complete List of Respondents to Survey Letter

The following people participated in the survey by answering the inquiry letter. Their knowledge and experience in this field was most helpful and their time and cooperation is appreciated.

1. Mr. G. H. Sprague, Design Engineer-Structures, The Martin Company, Orlando, Florida.

2. Professor James W. Mar, Assistant Professor of Aeronautical Engineering, Massachusetts Institute of Technology, Cambridge 39, Massachusetts.

3. Mr. J. W. Sweet, Chief Metallurgist, Boeing Airplane Company, Seattle 24, Washington.

4. Mr. M. Stone, Chief, Strength and Dynamics, Stability Section, Douglas Aircraft Company, Inc. , Long Beach Division, Long Beach, California.

5. Mr. Arthur Schnitt, Assistant Manager, Development Analysis Department, Research Division, Bell Aircraft Corporation, Buffalo 5, New York.

6. Mr. C. F. Berninger, Section Chief, Research and Advanced Development Division, AVCO Manufacturing Corporation.

7. Mr. E. P. Wheaton, Chief Missiles Engineer, Santa Monica Division, Douglas Aircraft Company, Santa Monica, California.

8. Mr. C. F. MacLean, Materials and Processes, Production Engineering Department, Lockheed Aircraft Corporation, Sunnyvale, California.

9. Mr. Ira. G. Hedrick, Chief Technical Engineer, Grumman Aircraft Engineering Corporation, Bethpage, Long Island, New York.

10. Mr. R. G. Wilson, Manager Advanced Engineering, North American Aviation, Inc. Missile Development Division, Downey, California.

Table X (Cont'd)

Complete List of Respondents to Survey Letter

11. Mr. V. G. Szebeholy, Manager, Advanced Structures Operations, General Electric Company, Ordnance Systems Department, Philadelphia 4, Pennsylvania.

12. Mr. L. L. Gilbert, Head, Materials Department, Liquid Engine Division, Aerojet-General Corporation, Azusa, California.

13. Mr. H. J. E. Reid, Director, National Advisory Committee for Aeronautics, Langley Aeronautical Laboratory, Langley Field, Virginia.

14. Rebecca H. Sparling, Design Specialist, Convair, Pomona, Calif.

15. Carl Lamb, Directorate of Research and Development Office, Deputy Chief of Staff, Department of the Air Force, Headquarters, United States Air Force, Washington 25, D. C.

16. Arnold B. Stein, Structures and Mechanics Laboratory, ABMA, Huntsville, Alabama

17. Oscar Holderer, Aeroballistic Laboratory, ABMA; Huntsville, Alabama.

18. Mr. I. E. Newlan, Chief, Reports Group, Jet Propulsion Lab. California Institute of Technology, Pasadena 3, California.

Table XI

METHODS OF CALCULATING THERMAL STRESS

Contained in Replies to the Survey Letter

Method	Company and Writer	Comments
Laminar	North American Aviation - Wilson Douglas - Wheaton	Methods about the same. Both incomplete.
Average	G. E. - Szebeholy	Not complete.
Classical	Avco - Berninger	Not complete.

METHODS OF CALCULATING ULTIMATE STRENGTH
WHEN THERMAL GRADIENTS ARE PRESENT

Method	Company and Writer	Comments
Laminar	Grumman - Hendrick	Used on plexiglass only but good method.
Laminar	Lockheed - MacLean	Not complete.
Inelastic Analysis	Martin - Sprague	Not complete. Good conclusions and observations.

When a section of the specimen with a thermal gradient is stressed above the proportional limit, the thermal stresses are decreased. This decrease in thermal stress is due to the yielding of the material. Several writers pointed out that the ultimate strength of a metal is not materially affected by the presence of thermal stresses. Sprague[2] of the Martin Company applied inelastic analysis methods to this problem. Several equations were given and theoretical results were compared with experimental results. He concluded that thermal stresses do not influence the static tensile failing load, but that inelastic behavior occurs at a reduced load level in the presence of thermal stress.

5.3 The Experimental Problems

After striving for several years to eliminate thermal gradients from test specimens, the problems of establishing controlled thermal gradients in the specimen were at first approached naively. But it was soon discovered that the magnitude of the desired gradients—up to 5000° F/in. — posed a new set of problems. A truly linear thermal gradient can be produced only by a uniform, unidirectional flow of heat. The direction of the thermal gradient is the same as the direction of the heat-flow, and the magnitude of the gradient is directly proportional to the magnitude of the heat-flow and inversely proportional to the thermal conductivity of the material in which the gradient is produced. For each 1000° F/in. of gradient in commonly available metallic materials, the required heat-flux density ranges from approximately 300 watts/sq in. for Inconel X to approximately 6000 watts/sq in. for copper. In order to reach even the lower end of this range, it was necessary to spend a large part of the effort on improving and evaluating the methods for heating one surface of the specimen, for cooling the opposite surface of the specimen, and for measuring the temperature of both surfaces to determine the magnitude of the gradient.

Induction heating, resistance heating, convection heating, and radiant heating were studied as means of introducing heat to the surface of the specimen.

An effort was made to utilize the "skin effect" of high-frequency induction heating to produce a thermal gradient in the metallic test piece. Since the depth of penetration of the induced currents becomes shallower

---

[2] Sprague, G. H., and Huang, P. C. "Behavior of Aircraft Structures Under Thermal Stress," presented at the SAE Aeronautical Meeting, Oct. 3, 1957.

with increasing frequency, a 3-megacycle, 4-kva generator was evaluated as a source to approximate surface heating. At the 3-megacycle frequency, the calculated depth of penetration was less than 0.001 in. for a ferromagnetic steel. Three types of special induction coils were designed and constructed to induce heating currents in a single flat surface rather than to encircle the whole work piece, as is customary. In each of the induction-heating experiments, the heat generated in the surface of the specimen was quite nonuniform and was insufficient to produce a gradient even approaching 1000° F/in. in steels. In nonmagnetic materials and even in ferromagnetic materials above the Currie point (about 1400° F for steel), the skin effect is much less intense, the depth of penetration increasing by a factor of several hundred due to the lower magnetic permeability.

Resistance heating was investigated because it would be very compatible with the existing equipment. Thermal gradients were measured using resistance heating with combinations of thermal insulation or radiant heat on the hot surface and air cooling or water cooling on the cooler surface. Thermal gradients typical of the resistance heating methods are shown graphically in Figure 23. where internal temperatures within the specimen are plotted as functions of the distance through the thickness. All of the variations with resistance heating produced nonlinear thermal gradients; but, if nonlinear thermal gradients were used in this program, the test results would be unnecessarily difficult to analyze and to compare with the theoretical calculations. Therefore, resistance heating was abandoned as a means of producing linear thermal gradients.

The most nearly linear thermal gradients are produced by heat from an external source introduced through one surface of the specimen either by conduction from a fluid medium or by radiation from an adjacent hot body. Calculations quickly showed that conduction from a gaseous medium could not be expected to give a sufficiently high heat input with any reasonable gas temperature. Conduction from a liquid medium would theoretically provide the best possible heat source, but the useful magnitudes of the gradients and of the hot-side temperatures would necessitate a molten salt or a molten metal as the heat-transfer medium. For these preliminary investigations, the initial cost of developing equipment for a liquid-salt or liquid-metal bath was not justified.

Four different sources of radiant energy were constructed and evaluated. An elliptical reflector-fixture was designed to focus the radiant energy from one 500-watt tubular quartz heating lamp onto one surface of a tensile specimen. In addition, a similar three-lobe fixture was built to focus the radiant energy from three lamps onto a single specimen. In both cases, the gradients, produced were insufficient for test purposes. A
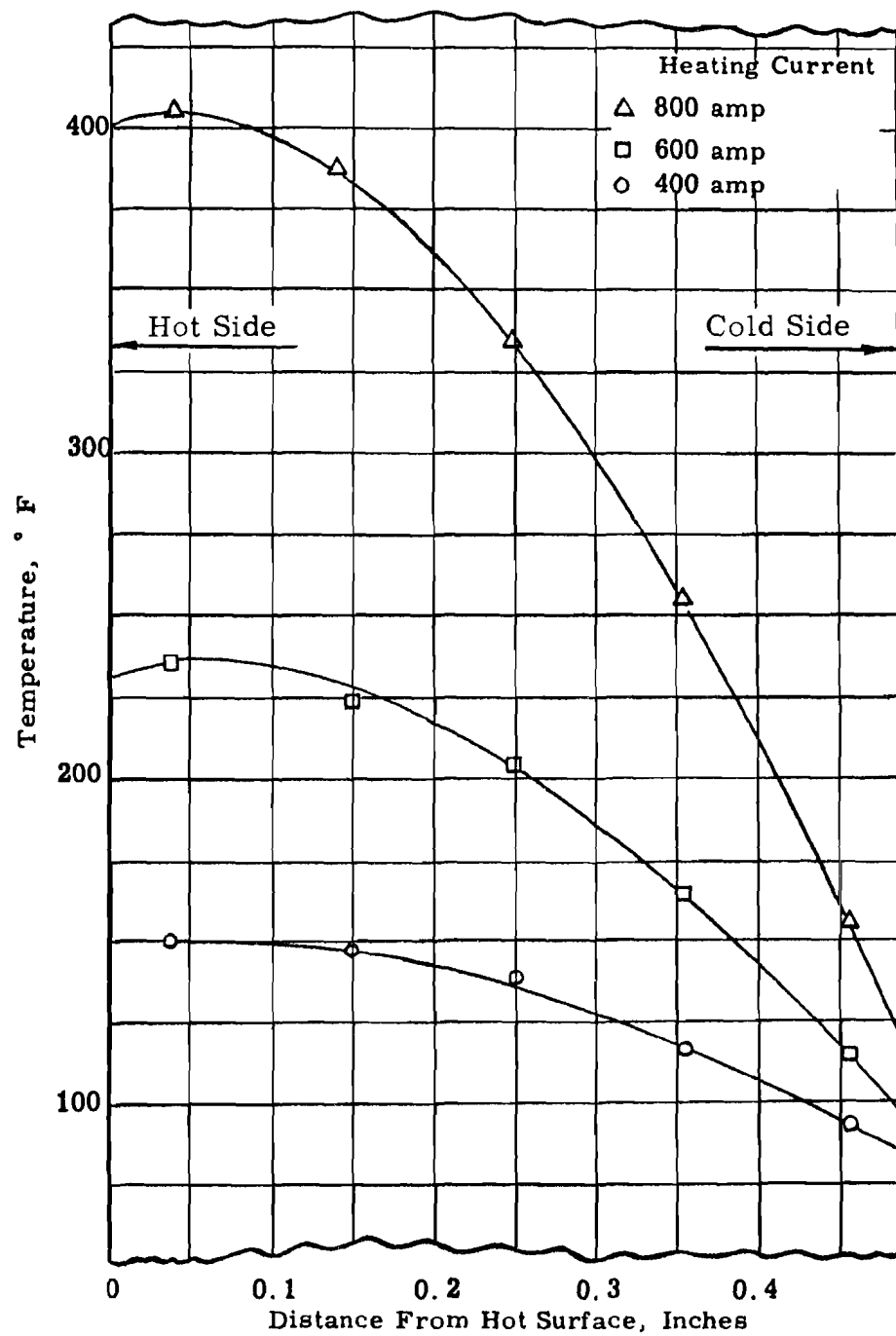
Figure 23. Thermal gradients produced by resistance heating. Hot side was thermally insulated; cold side was water cooled.

small carbon arc was substituted for the tungsten-quartz lamp in the single-lobe elliptical reflector. With 1/4 in. carbon electrodes, the measured power into the specimen was approximately the same as with the single lamp. The instability of the arc and the necessity for continually adjusting the electrodes are serious disadvantages of the arc source. The final source of radiant energy, which was used in the testing program, consisted of a resistance-heated strip of A-nickel, 3/4 in. wide by 1/16 in. thick, located parallel to the specimen about 1/16 in. away from one surface of the specimen.

Introducing sufficient heat into one surface of the specimen is only half of the general endeavor of producing large thermal gradients. A complementary problem of equal gravity is the efficient removal of heat from the cooler surface. Gaseous media would be convenient to use for cooling but suffer from the same deficiency as for heating—a large temperature drop in the surface film. Water was used as the cooling medium in the test program because of its favorable heat-transfer characteristics and its economy.

Early in the work with thermal gradients, it was learned that thermocouples welded to the surface of the specimen did not indicate the true surface temperature in the presence of high thermal gradients. The surface thermocouple wires were necessarily immersed in the cooling medium on one side and in the heating medium on the other side. Because the interfaces always have much poorer heat transfer than the metal specimen, there were large temperature differences between the surfaces of the specimen and the surrounding mediums. Being relatively good thermal conductors, the wires conducted heat either to or from the surface junction. The results of this heat flow in the thermocouple wires were erroneously high indications of temperature on the hot side and erroneously low indications on the cold side. For this reason the early measurements of thermal gradients were much higher than the true gradients, and the predictions were overly optimistic.

5.4 Special Equipment and Techniques

In order to accurately evaluate the methods of producing the gradients and the methods of measuring the gradients, a bar of 304 stainless steel, 1/2 in. x 1/2 in. x 12 in., was fitted with three thermocouple junctions of 0.005-in.-diameter wire imbedded in the bar, Figure 24. The three thermocouple junctions were centrally located in the bar in line with the direction of heat flow—one junction beneath the hot surface, one junction midway through the bar, and one junction beneath the cold surface. External

Stainless steel specimen

Surface thermocouples

Insulated thermo-
couple leads

Direction of heat flow

Steel clamping plate

Transite insulation
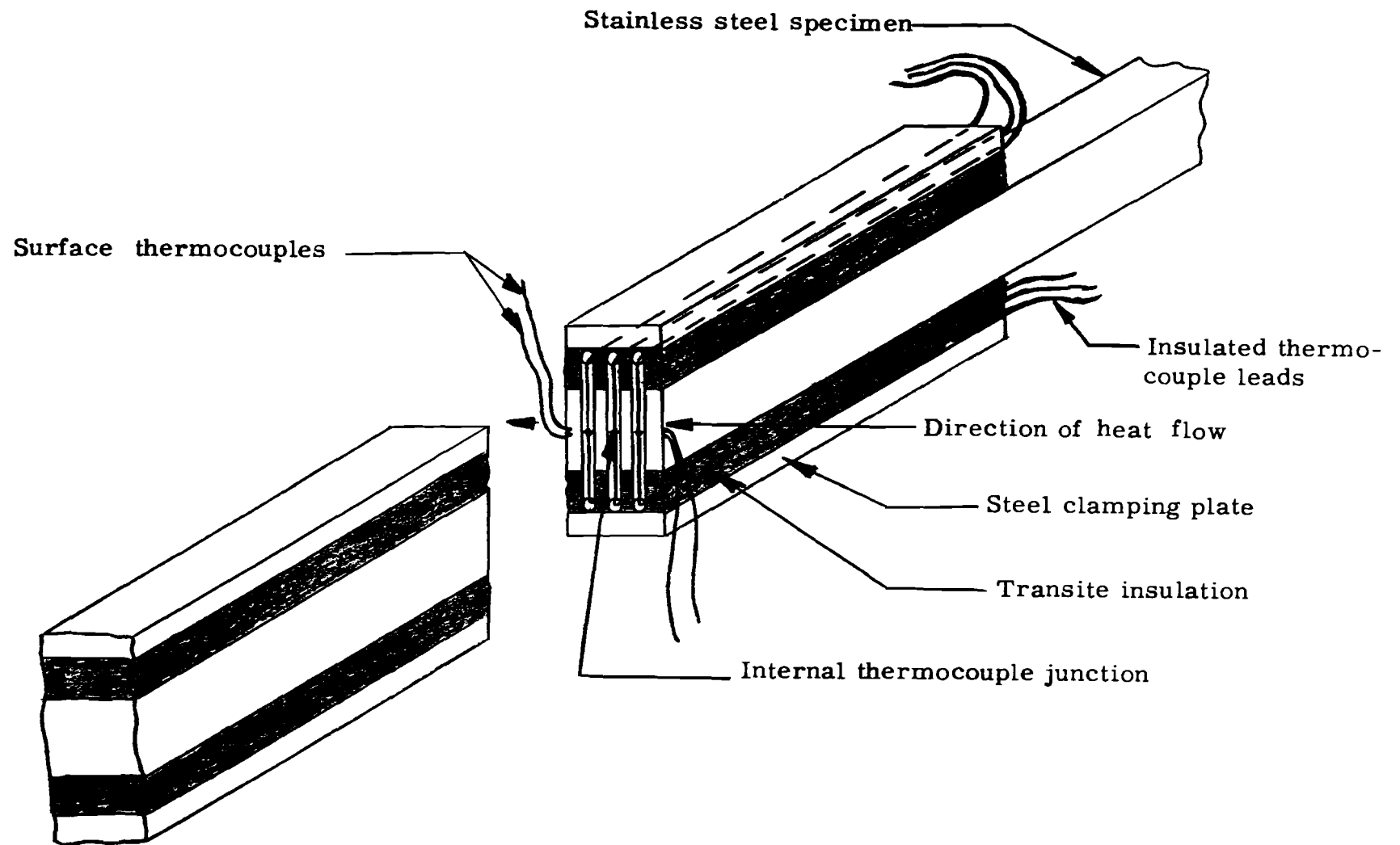
Internal thermocouple junction

Figure 24.   Sectioned view of special stainless steel specimen used to evaluate methods of
measuring thermal gradients.

thermocouples were welded to the hot and cold surfaces in line with the imbedded couples. For each method of producing thermal gradients, the temperature indications from each of the five thermocouples were plotted as functions of the position of the junction through the thickness of the bar in the direction of the heat flow. Each time that only external sources of heat were used, the points resulting from the three imbedded thermocouples delineated a straight line, the slope of which was assumed to represent the true linear temperature gradient through the bar. The true surface temperatures were obtained by extrapolating the straight line in both directions to the positions on the graph representing the hot and the cold surfaces. The points resulting from the surface thermocouples did not fall on the straight line; the hot-surface couple indicated a point above the line, and the cold-surface couple indicated a point below the line. Figure 25 shows two typical thermal-gradient curves obtained with the imbedded thermocouples and with surface thermocouples.

Since imbedded thermocouples would impair the strength of a tensile specimen, the problem became one of calibrating the surface thermocouples to indicate the true internal temperature gradient. Heat flow through thermocouple wires having been assumed to be the source of the error, the magnitude of the error should then bear some relationship to the size of the wire, and a theoretical zero-diameter wire should indicate the surface temperature with zero error. An attempt was made to approximate this theoretical zero-error situation by attaching to the surface of the specimen three thermocouples—all quite small but each a different size. Under conditions of large thermal gradients, the temperature indicated by each of the surface thermocouples was recorded and was plotted on a graph with temperature as the ordinate and cross sectional area of the wire as the abscissa. An extrapolation to zero cross section was planned to provide an accurate approximation to the true surface temperature and thereby to the true temperature gradient. Although the results of this experiment did bear out the basic assumption as to the source of error, the graph did not yield a simple linear function, which could be extrapolated reliably.

Since only a few test conditions and materials were planned for this preliminary test program with thermal gradients, a simple additive correction was determined for each test condition by observing the difference between the temperature indicated by the surface couples and the "true" surface temperature obtained from the extrapolation to each surface of the temperature gradient indicated by the three imbedded thermocouples. This correction was applied on each test to the measured temperatures, which were obtained from a single No. 36 chromel-alumel thermocouple junction welded to each of the two surfaces of the test specimen. Figure 26 is a graph of "true" surface temperature vs measured surface temperature for
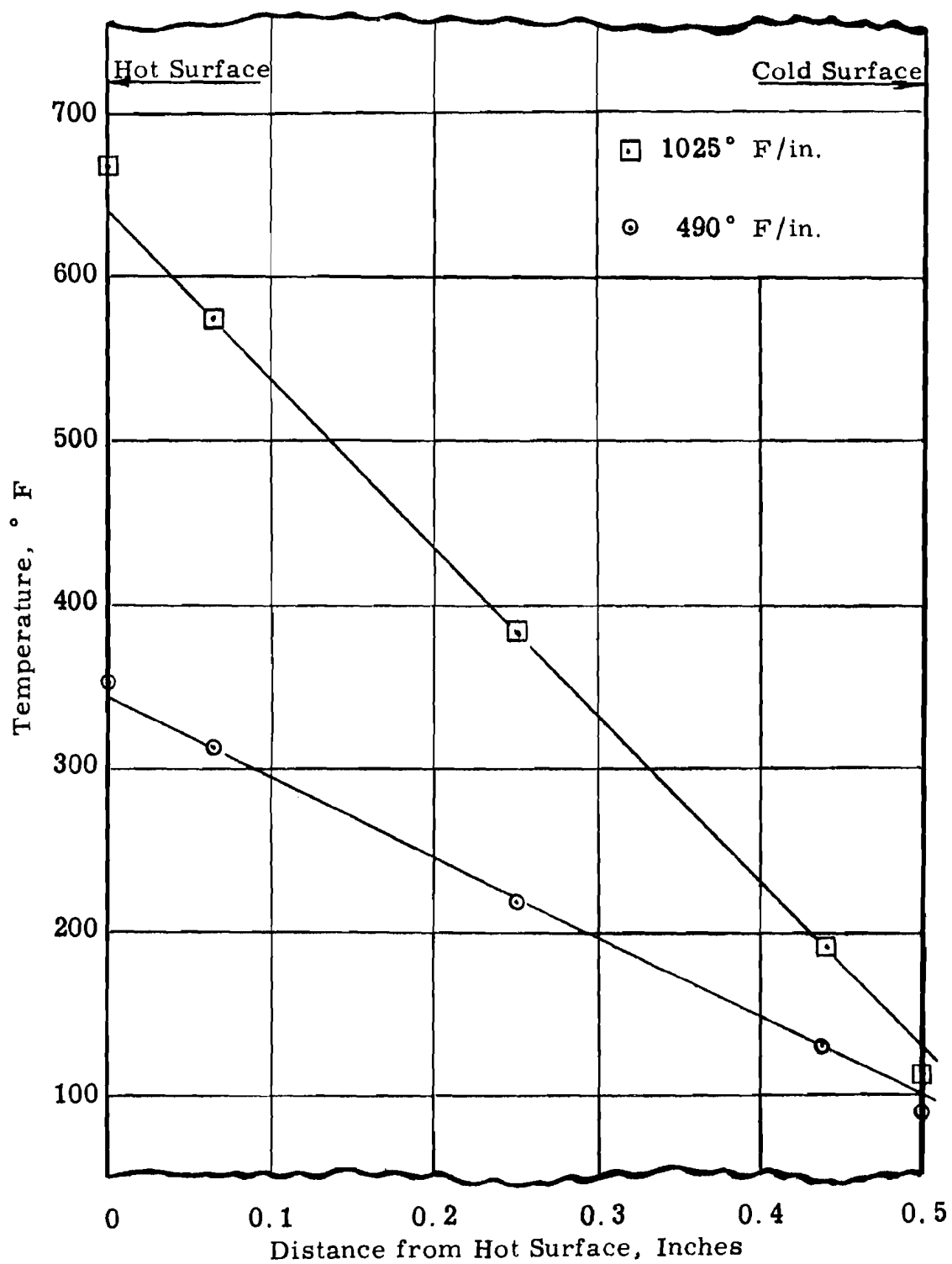
Figure 25. Typical thermal-gradient curves measured on the specimen
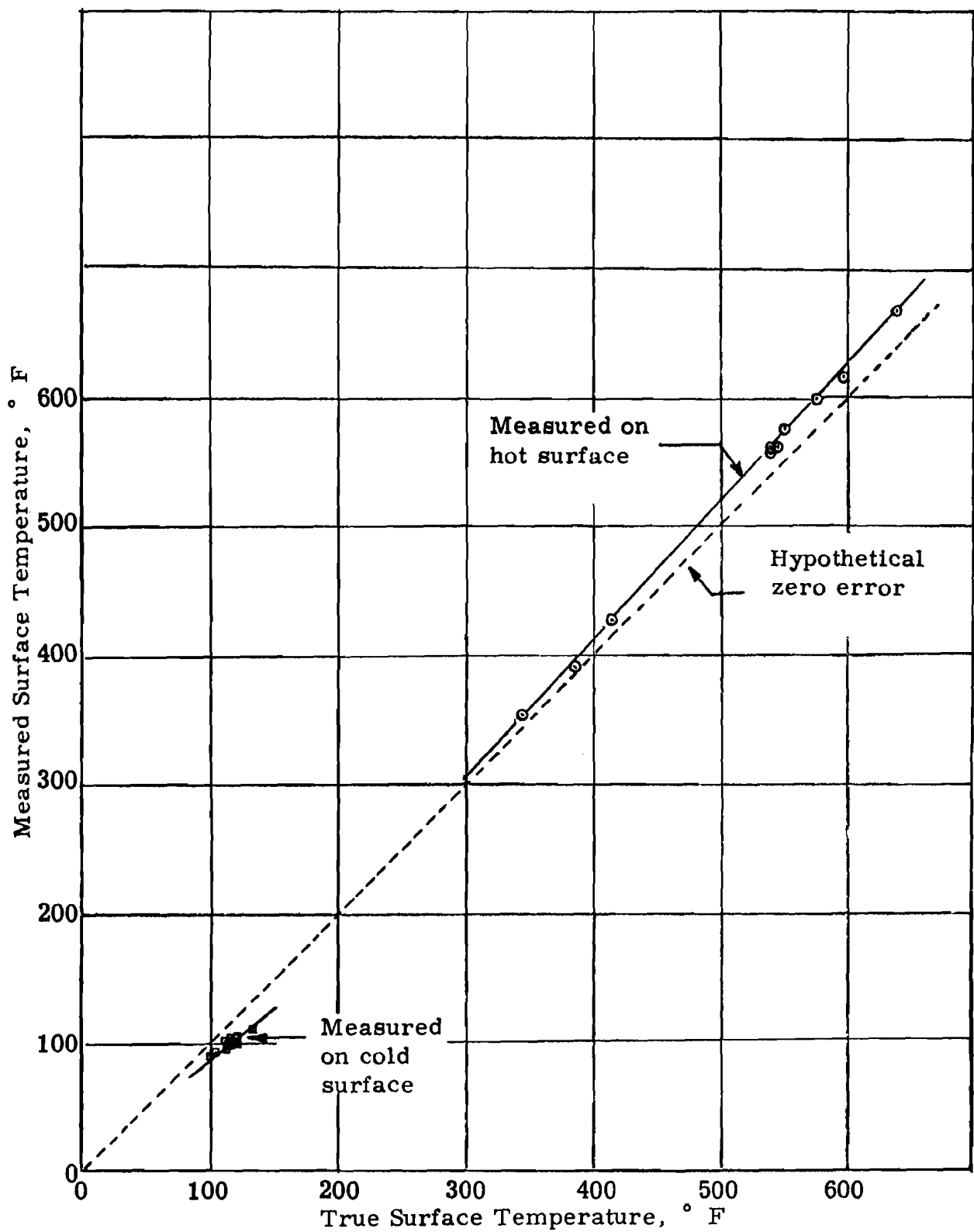with imbedded thermocouples and with surface thermocouples.

Figure 26. Measured surface temperature vs. true surface temperature. Corrections were obtained from this graph.

the final test conditions of water flow, heater size, and heater location. For each surface temperature measured during the tests, the corresponding correction was read graphically from Figure 26 (horizontal distance between the broken line and the solid line).

5.5 Test Procedure

The tensile specimens that were evaluated in the presence of thermal gradients were machined as shown in Figure 27 from annealed 17-7 PH stainless steel with a gage section 2 in. long by 0.3 in. wide by 3/16-in. thick. Each 3/16-in. thick edge was insulated with a 1/8-in. layer of Sauereisen cement to reduce heat losses from the edges and to prevent water from flowing around the edges to the hot side. The surface receiving heat was darkened to increase the radiant heat transfer to the specimen. A single thermocouple junction of No. 36 chromel-alumel wire was welded to each of the two active surfaces of the specimen.

A strip of A-nickel 3/4 in. wide by 1/16 in. thick was heated resistively and in turn radiated heat to the hot side of the specimen across a very short but uniform air gap. The pigtails, which normally supply the large heating current to the specimen, were connected to the lugs on the nickel heater strip. To insure uniform heating of the specimen, the heater-strip was made longer and wider than the gage section of the specimen. Asbestos-board supports mounted between the terminals prevented the heater from buckling. The heater was clamped to the specimen above the gage section. Asbestos spacers 1/16-in.-thick, placed at each end (outside the gage section) between the heater and the specimen, located the heater 1/16 in. from the specimen. The nickel strip was heated to about 2300° F by the same controlled source of heating current formerly used to heat tensile specimens. The heating current was controlled by an indication of temperature obtained from the thermocouple attached to the hot surface of the specimen.

A nozzle was fabricated to apply a uniform film of water to the cold side of the specimen. The outlet end of the nozzle was rectangular in shape and extended 1 in. past each end of the gage section of the specimen. The nozzle contained a central row of 1/64-in. holes extending the full length of the nozzle face. A clearance of 1/16 in. was maintained between the surface of the specimen and the perforated outlet end of the nozzle. A pressure regulator, a valve, and a flow meter was provided in the water-supply line to insure a uniform flow of water during the tests. A film of flowing water was formed between the nozzle and the specimen. A drain was provided below the lower specimen holder. The nozzle was clamped to the specimen
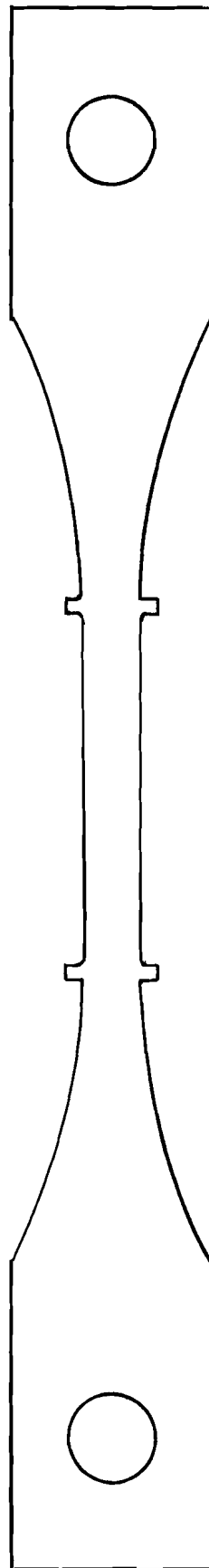
Annealed **17-7 PH** stainless
steel, **3/16** in. thick

Full Scale

Figure **27.** Tensile specimen for thermal-gradient evaluations.

above the gage section. Figure 28 shows a close-up photograph of the test specimen mounted in the tensile machine with the heater strip, the water nozzle, and the extensometer in place.

Tensile tests were made on eight specimens with thermal gradients ranging from 1200° F/in. to 1500° F/in. With the water regulated at the desired flow-rate the heater was slowly brought up to temperature. The specimens were loaded when the temperature of the hot surface had stabilized. A stress-strain curve was recorded for each test in the same manner and with the same equipment that was used for other short-time tensile tests in previous phases of this work. All tests were conducted at a nominal strain rate of 0.1 in./in./sec.

To assist in making comparisons between the results of the theoretical considerations and the results of the experimental determinations, several tests were conducted with uniform temperatures that corresponded to the average hot-side temperature (400° F), to the average cold-side temperature (125° F), and to the average center temperature (275° F).

5.6 Results and Discussion

The tensile properties of annealed 17-7 PH stainless steel are tabulated in Table XII for conditions of transverse thermal gradients ranging from 1200° F/in. to 1500° F/in. and for three uniform temperatures chosen to be representative of the hot side, the cold side, and the center of the specimens with the thermal gradients. In Figure 29 the average ultimate tensile strength and the average 0.2%-offset yield strength were plotted as functions of test temperature for the three uniform temperatures. For two thermal gradients—1260° F/in. and 1430° F/in.—the average experimentally determined ultimate strength and yield strength values were also plotted in Figure 29 at the mean temperature point on the abscissa. Finally on Figure 29, calculated values of ultimate and yield strength were plotted at the mean temperature point for a gradient of 1260° F/in. The calculated values were obtained from a method suggested by Mr. Ira G. Hedrick, Chief Technical Engineer, Grumman Aircraft Engineering Corp.

Of all the responses to the survey letter, only Mr. Hedrick's reply contained sufficient detail to be carried through to completion. According to this method the sample was imaginatively divided into laminae, and each lamina was assigned a strength according to its temperature. The strength assignments were interpolated from the curves of Figure 29 for the uniformly heated specimens. The strength of the sample was taken as the sum of the strengths of the laminae. The same procedure was used to calculate the values of ultimate and yield strength plotted on Figure 29.
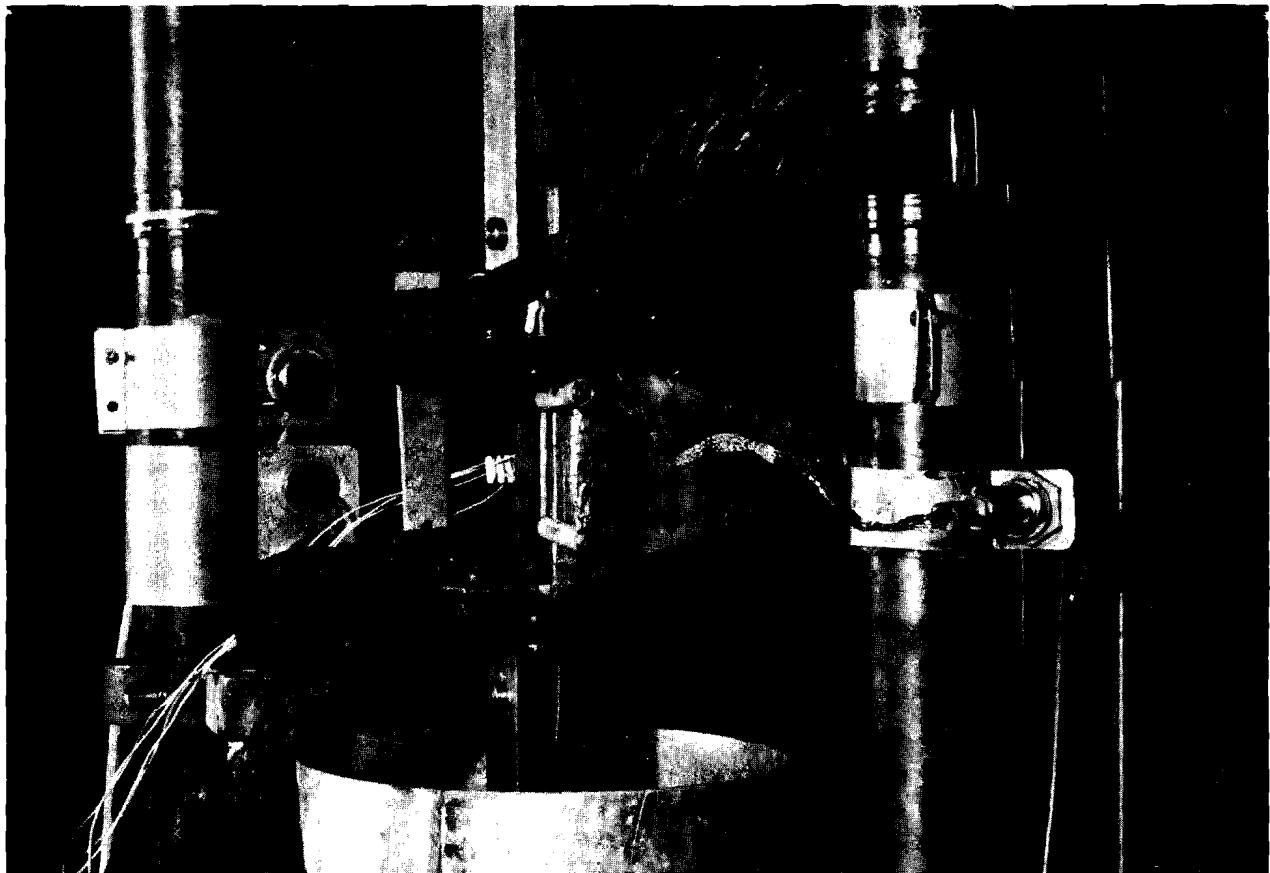
Figure 28. A close-up photograph of the assembled apparatus for producing large controlled thermal gradient in a tensile specimen.
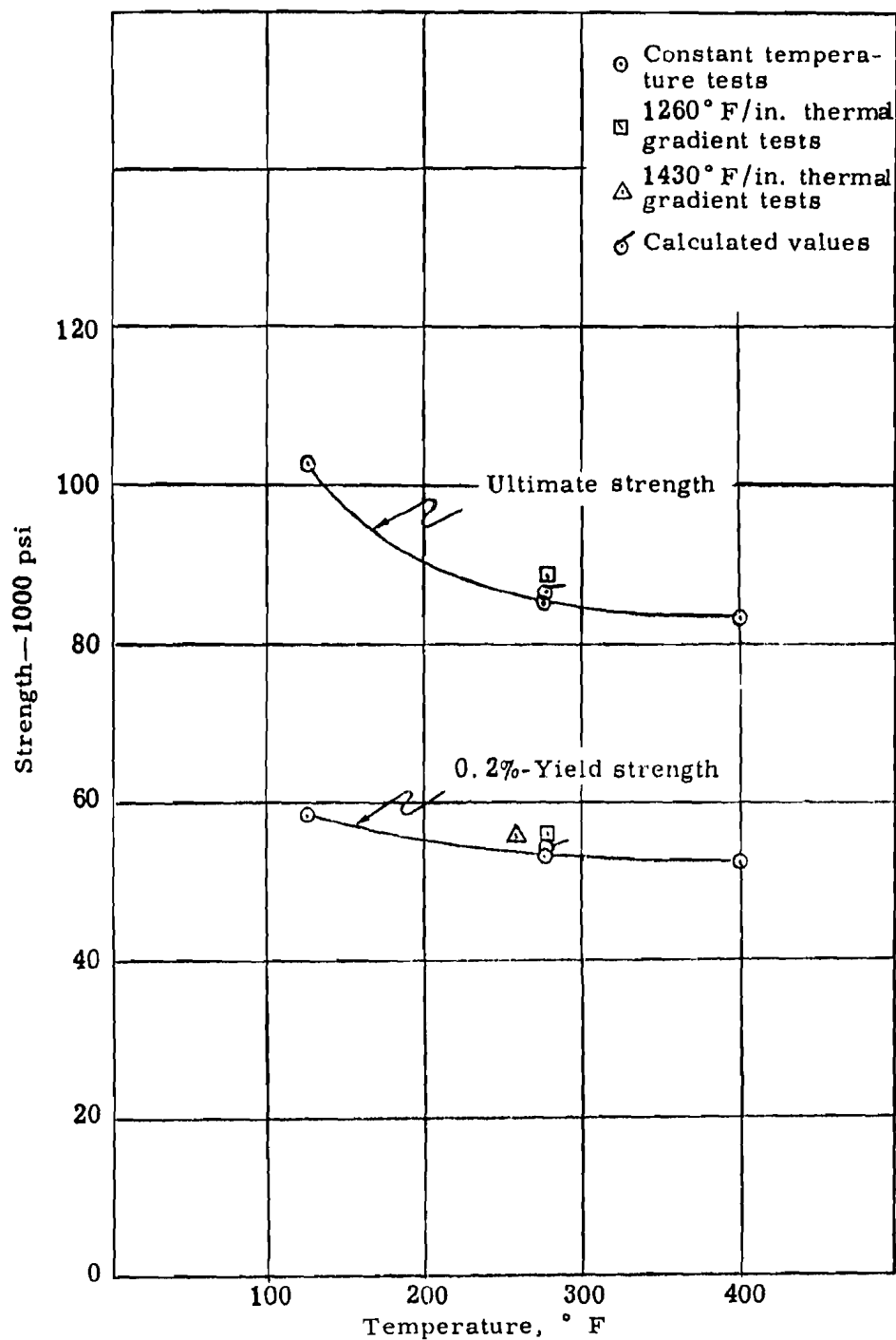
Figure 29. Comparison of ultimate tensile strength and 0. 2%-
offset yield strength (1) from tests with constant
temperature, (2) from tests with two levels of
thermal gradient and (3) from calculations for
similar thermal gradients.

Table XII

Tensile Properties of Annealed 17-7 PH Stainless Steel with Controlled Thermal
Gradients and with Uniform Temperatures

Temperature, ° F			Gradient ° F/In.	Strength, 1000 psi		Percent Elongation in 2 in.
Hot Side	Cold Side	Average		Ultimate	0.2%-Offset Yield	
400	160	280	1200	—	55.2	24.0
400	141	270	1300	—	55.5	22.0
400	155	277	1290	—	55.6	25.0
402	160	281	1220	87.8	—	24.0
400	150	275	1290	89.8	—	23.0
Avg 400	153	277	1260	88.8	55.7	23.6
397	124	260	1380	—	56.4	37.5
403	124	263	1400	—	53.8	29.5
402	102	252	1500	—	55.8	33.0
Avg 401	117	258	1427		55.3	33.3
—	—	400	None	84.1	—	24.0
—	—	400	None	82.3	—	26.0
—	—	400	None	—	53.6	27.0
—	—	400	None	—	51.3	26.0
Avg		400		83.2	52.4	25.8
—	—	125	None	—	58.0	36.0
—	—	125	None	—	58.9	36.0
—	—	125	None	104.3	—	34.5
—	—	125	None	101.3	—	38.5
Avg	—	125		102.8	58.5	36.3
—	—	275	None	85.3	53.1	27.5
—	—	275	None	84.8	53.1	27.2
Avg		275		85.1	53.1	27.4

5.7 Conclusions

The curves and points on Figure **29** show that both the ultimate strength and the yield strength depend primarily upon the mean temperature and show very little dependence upon transverse temperature-gradients up to **1430°** F/ in. A spread of less than **5%** was obtained both on the yield strength values and on the ultimate strength values obtained by three different methods—**(1)** tensile tests with thermal gradients, **(2)** tensile tests with uniform temperature equal to mean temperature of the thermal-gradient test, and **(3)** calculations of strength values for a similar thermal gradient. For purposes of design data, tests with thermal gradients within the limited range of this work do not appear to justify the additional expenditure for time and equipment, because results of sufficient accuracy can be obtained from conventional elevated-temperature tensile data.

The strength of materials in the presence of thermal gradients is probably influenced significantly by at least two other factors not investigated in this work. The mean temperature and the thickness of the material may be important whenever the maximum temperature is pushed up into the range where the strength deteriorates rapidly with further increase in temperature. In other words, the maximum temperature or the temperature differential in terms of ° F is probably more significant than the temperature gradient in terms of ° F/in.

One of the most valuable results of this work was the evaluation of surface thermocouples for measuring thermal gradients. Many investigators have used the temperatures measured with surface thermocouples to deter- mine temperature gradients, but the results of this investigation challenge the validity of that method.